AD-A060 485 BATTELLE COLUMBUS LABS OHIO F/G 9/5
DIELECTRIC GRATING ANTENNAS.(U)
JUL 78 S T PENG, F SCHWERING DAAG29-76-D-0100
UNCLASSIFIED CORADCOM-78-3 NL

1 OF 1
AD A060 485

END
DATE FILMED
1-79
DDC

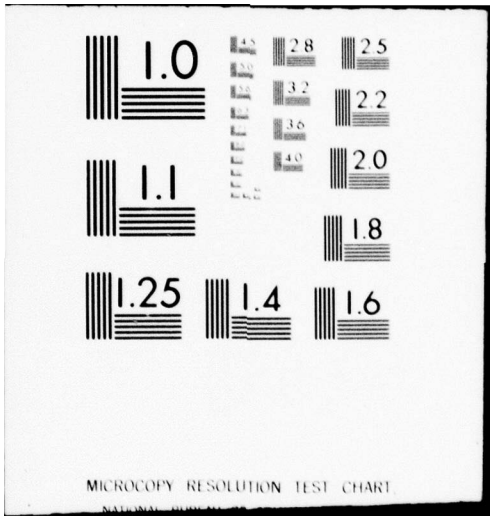
1.0
1.1
1.25
1.4
1.6
1.8
2.0
2.2
2.5
2.8
3.2
3.6
4.0
MICROCOPY RESOLUTION TEST CHART

RESEARCH AND DEVELOPMENT TECHNICAL REPORT
CORADCOM- 78-3

DIELECTRIC GRATING ANTENNAS

S.T. Peng
DEPARTMENT OF ELECTRICAL ENGINEERING
POLYTECHNIC INSTITUTE OF NEW YORK

F. Schwering
CENTER FOR COMMUNICATIONS SYSTEMS

July 1978

CORADCOM
US ARMY COMMUNICATION RESEARCH & DEVELOPMENT COMMAND
FORT MONMOUTH, NEW JERSEY 07703

NOTICES

Disclaimers

The citation of trade names and names of manufacturers in this report is not to be construed as official Government indorsement or approval of commercial products or services referenced herein.

Disposition

Destroy this report when it is no longer needed. Do not return it to the originator.

UNCLASSIFIED

SECURITY CLASSIFICATION OF THIS PAGE (When Data Entered)

REPORT DOCUMENTATION PAGE

READ INSTRUCTIONS BEFORE COMPLETING FORM

1. REPORT NUMBER: CORADCOM-78-3	2. GOVT ACCESSION NO. / 3. RECIPIENT'S CATALOG NUMBER
4. TITLE (and Subtitle): DIELECTRIC GRATING ANTENNAS,	5. TYPE OF REPORT & PERIOD COVERED
	6. PERFORMING ORG. REPORT NUMBER
7. AUTHOR(s): S. T. Peng and F. Schwering	8. CONTRACT OR GRANT NUMBER(s): DAAG29-76-D-0100
9. PERFORMING ORGANIZATION NAME AND ADDRESS: CENCOMS, DRDCO-COM-RH, Fort Monmouth, NJ 07703	10. PROGRAM ELEMENT, PROJECT, TASK AREA & WORK UNIT NUMBERS: ILI 611102.H48.H2.11.01
11. CONTROLLING OFFICE NAME AND ADDRESS: CENCOMS/CORADCOM, Fort Monmouth, NJ 07703	12. REPORT DATE: July 1978 / 13. NUMBER OF PAGES: 57
14. MONITORING AGENCY NAME & ADDRESS (if different from Controlling Office): 1L161102AH48	15. SECURITY CLASS. (of this report): Unclassified / 15a. DECLASSIFICATION/DOWNGRADING SCHEDULE
16. DISTRIBUTION STATEMENT (of this Report): Approved for public release; distribution unlimited	17. H2
12. 78p.	
17. DISTRIBUTION STATEMENT (of the abstract entered in Block 20, if different from Report)	9. Research and development technical rept.,
18. SUPPLEMENTARY NOTES	

19. KEY WORDS (Continue on reverse side if necessary and identify by block number)

mm-wave antennas; periodic dielectric surface wave guide; periodic dielectric antennas; leaky wave guide antenna theory

15. DAAG29-76-D-0100

20. ABSTRACT (Continue on reverse side if necessary and identify by block number)

We present in this report a comprehensive and systematic study of dielectric grating antennas for use in millimeter wave systems. First of all, the feasibility of grating surface-wave structures for use as millimeter wave antennas is positively established on the basis of extensive numerical data for the case of infinitely wide gratings with uniform surface wave excitation at normal incidence. Secondly, a new approximation technique is introduced to obtain analytic formulas that are simple and useful for the practical design of grating antennas. Thirdly, the results for the normal incidence case are extended to the general-

DD FORM 1 JAN 73 1473 EDITION OF 1 NOV 65 IS OBSOLETE

UNCLASSIFIED

SECURITY CLASSIFICATION OF THIS PAGE (When Data Entered)

case of oblique incidence, so that antennas of finite width can be rigorously investigated.

TABLE OF CONTENTS

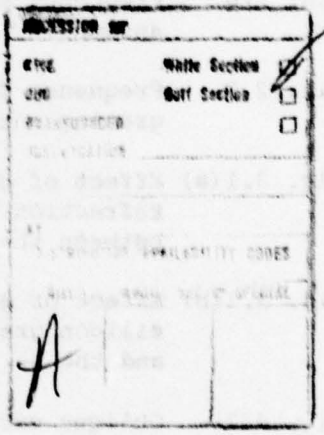

LIST OF FIGURES

SUMMARY

We present in this report a comprehensive and systematic study of dielectric grating antennas for use in millimeter wave systems. First of all, the feasibility of grating surface-wave structures for use as millimeter wave antennas is positively established on the basis of extensive numerical data for the case of infinitely wide gratings with uniform surface wave excitation at normal incidence. Secondly, a new approximation technique is introduced to obtain analytic formulas that are simple and useful for the practical design of grating antennas. Thirdly, the results for the normal incidence case are extended to the general case of oblique incidence, so that antennas of finite width can be rigorously investigated.

The feasibility study of millimeter wave grating antennas was based on an exact formulation of periodic dielectric waveguides as an electromagnetic boundary value problem that was carried out by the author (a reprint of a published paper [1] is included as the appendix in this report). Preliminary considerations and criteria for the design of grating antennas are discussed on the basis of well known surface wave characteristics of uniform dielectric waveguides and the basic principle of radiation from a periodic structure. For properly chosen structure parameters, extensive numerical data were obtained to determine the effect of grating period and thickness and the frequency scanning characteristics of a radiating beam. Three different materials of interest for millimeter wave applications are considered; they are: Silicon ($\varepsilon = 12$), $A\ell_2O_3$ ($\varepsilon = 10$) and Boronitride ($\varepsilon = 4$). We have determined that silicon and $A\ell_2O_3$ grating structures can produce a sufficiently large radiation constant to meet the special requirements of millimeter wave systems, but not boronitride grating structures. For both silicon and $A\ell_2O_3$ gratings, it is shown that a ten percent change in wavelength may yield a scanning angle of about 20° in either forward or backward direction.

The new approximation technique introduced here possesses two advantages over those previously employed for the analysis of optical periodic couplers: (1) the analysis is based on the perturbation introduced by the

periodic layer on the dispersion relation of well known surface waves; such an approach will yield directly the radiation constant of the grating antenna; (2) the perturbation term is cast into the form of a variational expression, so that a first order approximation of the initial field should give rise to only a second order effect on the accuracy of a dispersion root. This new approximation technique is applicable to gratings of large dielectric constant and will be particularly useful for analysis of millimeter wave grating antennas.

The general case of oblique incidence is a three-dimensional (vector) boundary value problem that supports only hybrid modes; it requires the coupling of "TE and "TM" modes. We have carried out an exact formulation of such a vector boundary value problem, rigorously taking into account the effect of coupling between the two modes. The analysis includes the scattering of a plane wave by a grating structure under the most general condition. This paves the way for future research on grating antennas of finite width.

I. INTRODUCTION

Recent advances in the fabrication of millimeter (mm)-wave systems using the integrated circuit (IC) technology have stimulated considerable interest in the development of new components and devices for signal generation, transmission and processing involving mm-waves. To be compatible with the IC technology, it is essential that an antenna structure may also be integrated with other components, so that the cost, size and weight of the antenna can be greatly reduced. This work is intended to study electromagnetic characteristics of a potential antenna structure that will be compatible with the IC technology for mm-wave applications.

The potential antenna structure envisioned here is a dielectric grating in conjunction with an open dielectric waveguide, which belongs to the general class of traveling wave antennas. Such a composite waveguide structure has been generally called a periodic dielectric waveguide, because it may also perform, with proper designs, many other functions, such as the filtering and the distributed feedback of electromagnetic waves. As a rigorous electromagnetic boundary value problem, the periodic dielectric waveguide structure has been extensively analyzed in the past, mostly in the context of integrated optics applications. The purpose of this work, however, is to investigate the periodic dielectric waveguide with physical and structural parameters that are pertinent to applications in the mm-wave frequency range and with a particular attention directed toward the radiation characteristics of such a structure as an antenna. For simplicity and to emphasize the main aspect of interest here, the periodic dielectric waveguide will also be referred to as a dielectric grating antenna or simply grating antenna.

As an exact electromagnetic boundary value problem, periodic dielectric waveguides have been rigorously formulated for the case of normal incidence (with respect to the grating grooves) and with assumptions that both the structure

and the source distribution are invariant along the grooves. Under these simplifying conditions, a general electromagnetic wave can be decomposed into the two independent TE and TM modes, which have been extensively analyzed in the literature. The advantage of such an exact formulation is that it applies to gratings of arbitrary structural parameters. On the other hand, the exact formulation has to rely on final numerical results (by using a high speed and high capacity computer) for physical interpretations of wave phenomena associated with the periodic waveguide. For gratings of relatively low dielectric constant (close to that of air), a perturbation technique has been introduced to obtain approximate analytic results that are very simple and useful for practical design of optical periodic couplers. Thus, for most optical applications, the exact and approximate analyses may be used complementarily, as situations require.

Grating antennas for mm-wave applications differ from those for optical couplers in many respects. Because of the longer wavelength, the limitation on the size of grating antennas is very severe. For example, at the frequency of 100 GHz, an antenna of 3 inches in length permits only about 25 wavelengths in free space. To radiate all the incoming energy within 25 wavelengths (in contrast to more than 1000 wavelengths for optical couplers) require a very large leakage constant of the periodic waveguide. Although the high dielectric constants of mm-wave materials are very helpful for achieving a large leakage constant, they cause numerical difficulties in an exact analysis of the antenna. Also, the previously developed perturbation analysis that was based on the small difference in the dielectric constants of the grating does not yield sufficiently accurate results and a new approximation technique has to be introduced to obtain better analytic results for dielectric grating antennas of high dielectric constant.

While the simplifying conditions that both the structure and the source of excitation are uniform along the grooves hold for most optical couplers, they are too restrictive for applications to mm-wave grating antennas. Our preliminary

analysis has concluded that to investigate the effect of finite grating width, the most basic problem to be solved is the guiding of waves propagating at an oblique angle in an infinitely wide grating. This is a three dimensional electromagnetic boundary value problem that supports only hybrid modes, e.g., it requires the coupling between TE and TM modes. Such a vector boundary value problem has not been formulated so far, because of its mathematical difficulties and lack of practical interest in the past. For grating antennas of finite width, however, a thorough understanding of the vector boundary value problem is essential and remains to be carried out.

To summarize, we have identified three important basic problems that need to be analyzed, before a comprehensive and systematic study of dielectric grating antennas can be made. First of all, extensive numerical data for the simple case of normal incidence have to be obtained in order to determine the feasibility of the periodic surface waveguide as an antenna structure. Secondly, if feasible, approximation techniques need to be introduced to obtain analytic formulas that are simple and useful for practical design purposes. Thirdly, the results for the normal incidence case have to be extended to the oblique incidence case, so that antennas of finite width can be rigorously investigated. Under the Laboratory Research Cooperative Program (LRCP; during July and August, 1977), the first basic problem has been successfully carried out by using a computer program (previously developed by the author for optical periodic couplers) that is based on the exact formulation of the periodic dielectric waveguide as an electromagnetic boundary value problem. The results are given and explained in Section II; they confirm that silicon and aluminum oxide grating waveguides can indeed be used as mm-wave antennas with versatile radiation characteristics. In addition, a new approximation technique that holds for grating antennas with a high dielectric constant has been developed in Section III and an exact formulation for the oblique incidence case has been carried out in Section IV. It should be emphasized, how-

ever, that within the limit of two months under the LRCP, the second and third basic problems have been analyzed only in principle, and further work remains to be done in the future.

II. EXACT ANALYSIS

In the case of normal incidence of a surface wave to a grating of infinite width, the electromagnetic fields are invariant along the groove (in the y-direction) and we have a two-dimensional boundary value problem in which the TE and TM modes exist independently and can thus be considered separately. The formulation of such a boundary value problem has been previously carried out and published in the literature by the present author [1], of which a reprint is included as Appendix A for reference in this report. Also, for mm-wave applications, the case of oblique incidence will be of more practical interest and is formulated under the most general conditions in Section IV. Therefore, it is unnecessary to repeat here the formulation for the special case of normal incidence.

The exact formulation of the grating antenna with rectangular grooves as an electromagnetic boundary value problem remains the only reliable approach under the most general conditions. As an exploratory study of grating antenna for mm-wave applications, it is logical to begin with the special case of normal incidence, of which an elaborate computer program has already been developed by the author, in conjunction with optical periodic couplers in the past. We present here the numerical results of grating antennas pertinent to mm-wave applications.

A. Surface Waves of a Uniform Dielectric Waveguide

Before embarking on an elaborate numerical analysis for a grating antenna, we present first some propagating characteristics of surface waves supported by a uniform dielectric waveguide which may be taken as a limiting case of periodic dielectric waveguide with a vanishing thickness of the grating. For simplicity, a surface wave supported by a uniform dielectric waveguide will be henceforth called a basic surface wave. The analysis of basic surface waves is simple and well understood; the results are given here, in the form of curves, for two purposes: one is that they provide the necessary initial conditions for an elaborate

numerical analysis of grating antennas and the other is that they can be used for some preliminary designs of grating antennas without extensive numerical analysis.

A uniform dielectric waveguide that is relevant to the problem of grating antennas for mm-wave applications is depicted in Fig. 2.1. The structure consists of a dielectric film on a ground plane in the free space where the dielectric constant is equal to unity. It is well known that such a structure supports both TE and TM surface wave modes. In order to avoid the ohmic loss in the ground plane, TM modes are more desirable in practice than TE modes. Therefore, we shall consider only the TM modes in the present study.

For a given film material, the characteristics of basic surface waves depend only on the ratio t_f/λ where λ is the free-space wavelength. The normalized longitudinal propagation constant of the surface wave or the effective index of refraction, $n_{eff} = \beta_{sw}/k_o$, is plotted against t_f/λ as dispersion curves in Fig. 2.2, for silicon, aluminum oxide, and boronitride as the film material. Although only the fundamental mode, $m = 0$, will be considered for mm-wave antenna applications, higher mode dispersion curves are also included so that we may choose the thickness of the film to ensure the single mode operation.

Once the longitudinal propagation constant of a surface wave in a uniform waveguide is determined, all quantities associated with the surface wave are easily determined. In particular, the transverse decay constant in the air region is given by:

$$\gamma_a = k_o(n_{eff}^2 - 1)^{1/2} \qquad (2.1)$$

where k_o is the propagation constant of plane wave in the free space. Evidently, the larger the effective index of refraction, n_{eff}, the larger the decay constant in air and the more the surface-wave energy is confined within the film. Figure 2.2(c) shows that there exist an intermediate frequency range where the surface-wave characteristics changes most rapidly with the change in frequency.

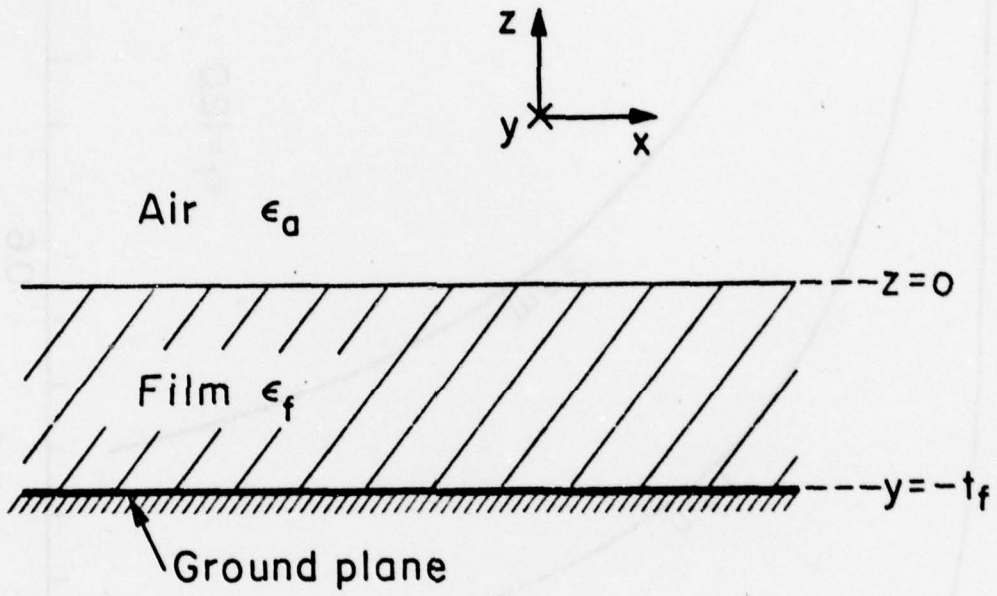

Fig. 2.1. Single dielectric film on a ground plane.

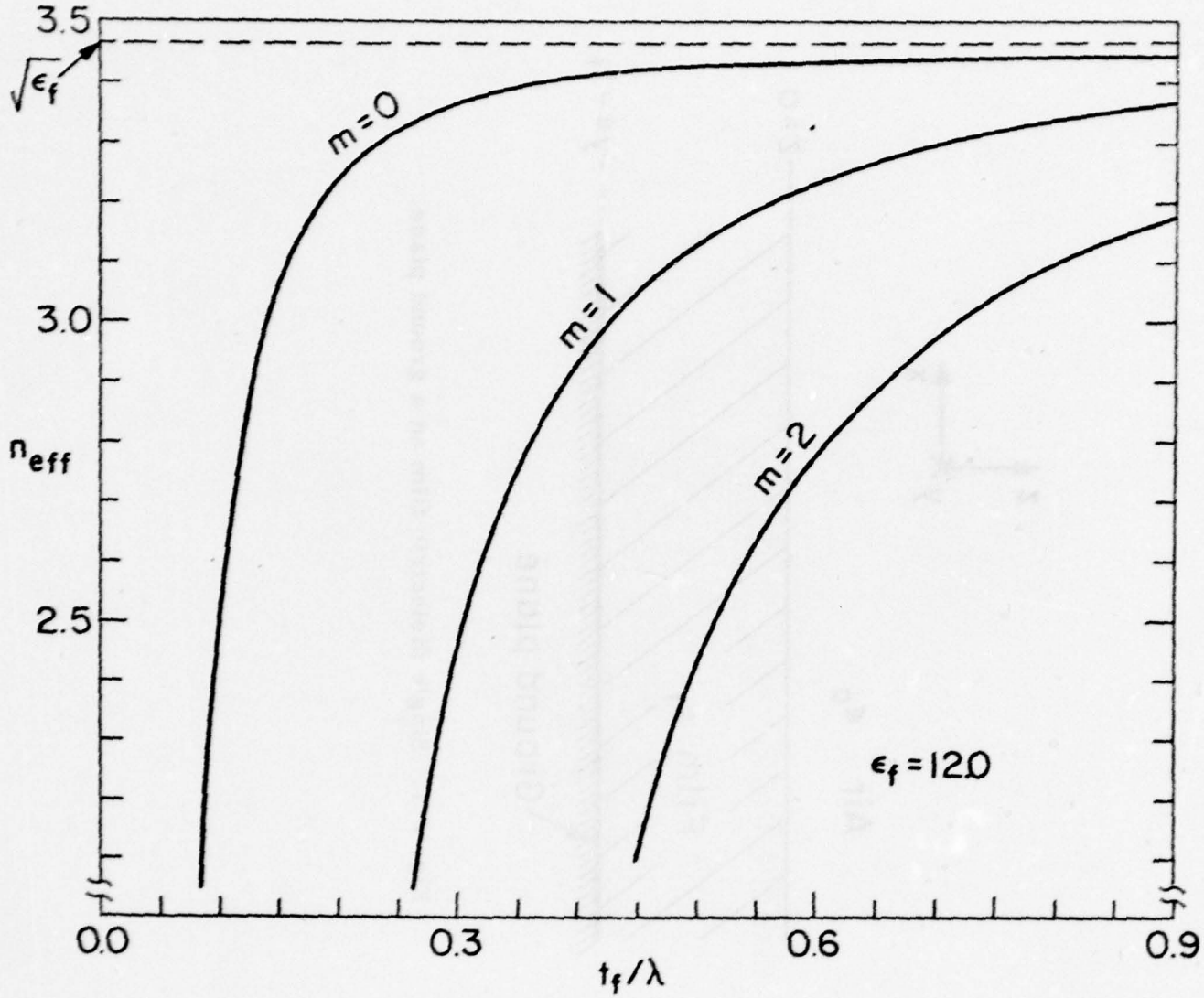

Fig. 2.2(a). Dispersion curves of uniform silicon waveguide.

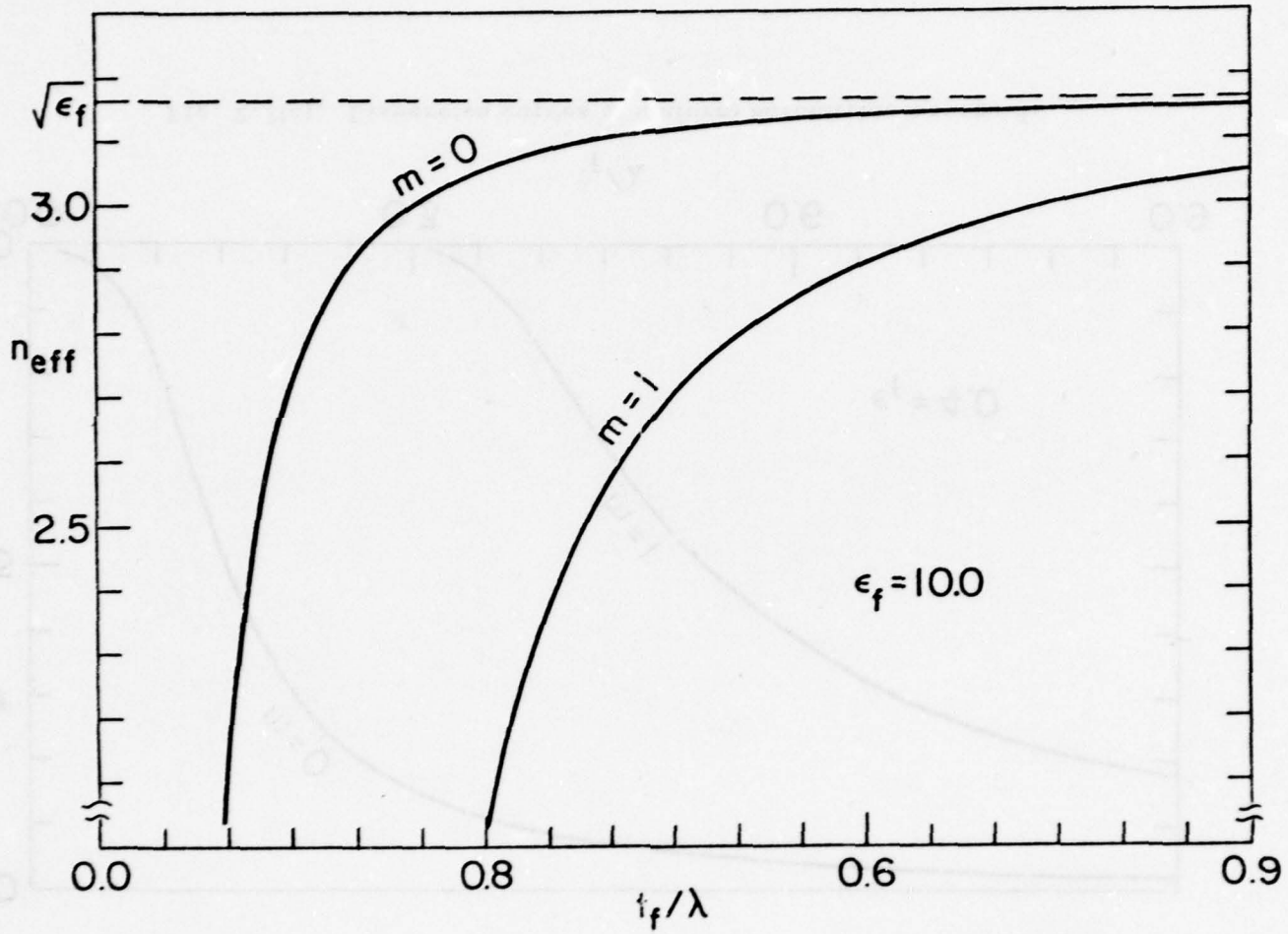

Fig. 2.2(b). Dispersion curves of uniform aluminum oxide waveguide.

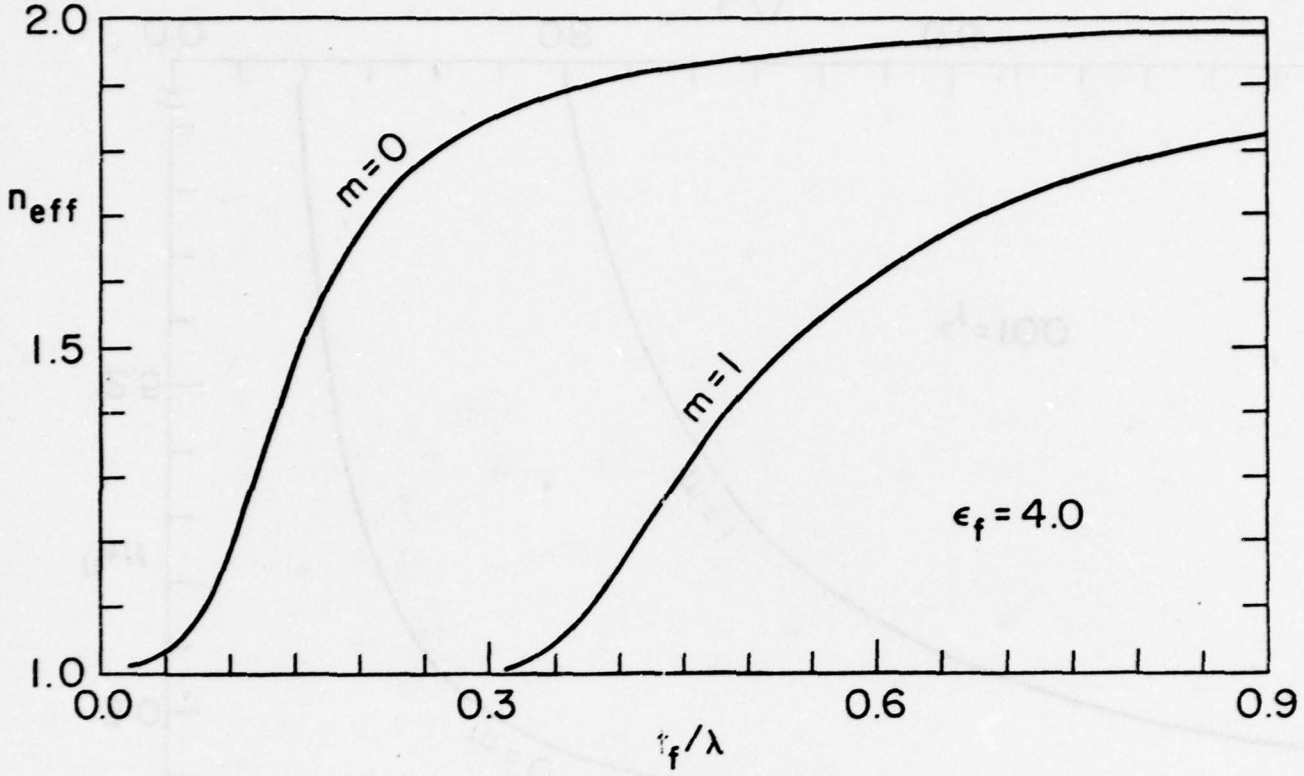

Fig. 2.2(c). Dispersion curves of uniform boronitride waveguide.

The same is true in Figs. 2.2(a) and (b) in which the portion of small t_f/λ is omitted. These physical concepts will be important to the design of grating antennas, as we shall further discuss in what follows.

B. Grating Antenna

The configuration of a dielectric grating antenna structure is shown in Fig. 2.3. Such an electromagnetic structure has been previously analyzed in the context of optical periodic couplers [1] and many radiation characteristics of the structure have been known. For example, it is well known that the radiation is the strongest when the groove width is nearly equal to the tooth width. For this reason, we shall choose throughout this work the width of the grooves to be equal to that of the teeth, as shown in Fig. 2.3. Conceptually, we shall regard the portion between $z = 0$ and $z = -t_f$ to be the uniform film region and the portion between $z = 0$ and $z = t_g$ to be the grating region; the radiation of the grating antenna will then be taken to be due to the periodic perturbation of the grating on the surface wave guided by the uniform film. It is noted that our analysis here will be restricted to the structural configuration shown in Fig. 2.3, although the formulation and the computer program for the boundary value problem apply equally well to more general configurations, such as the grating teeth having a dielectric constant different from that of the film. Therefore, for a given dielectric material, the antenna structure is characterized by the three parameters: the thickness of the uniform film, t_f, the thickness of the grating region, t_g, and the period of the grating, d. In addition, the frequency of a source is characterized by the wavelength, λ. We shall determine the effect of each of the four parameters on the characteristics of the antenna.

Because of the periodicity of the grating antenna, the electromagnetic fields everywhere must consist of all the space harmonics. For TM modes, we have:

$$H_y(x, z) = \sum_n I_n(z) \exp(i k_{xn} x) \qquad (2.2)$$

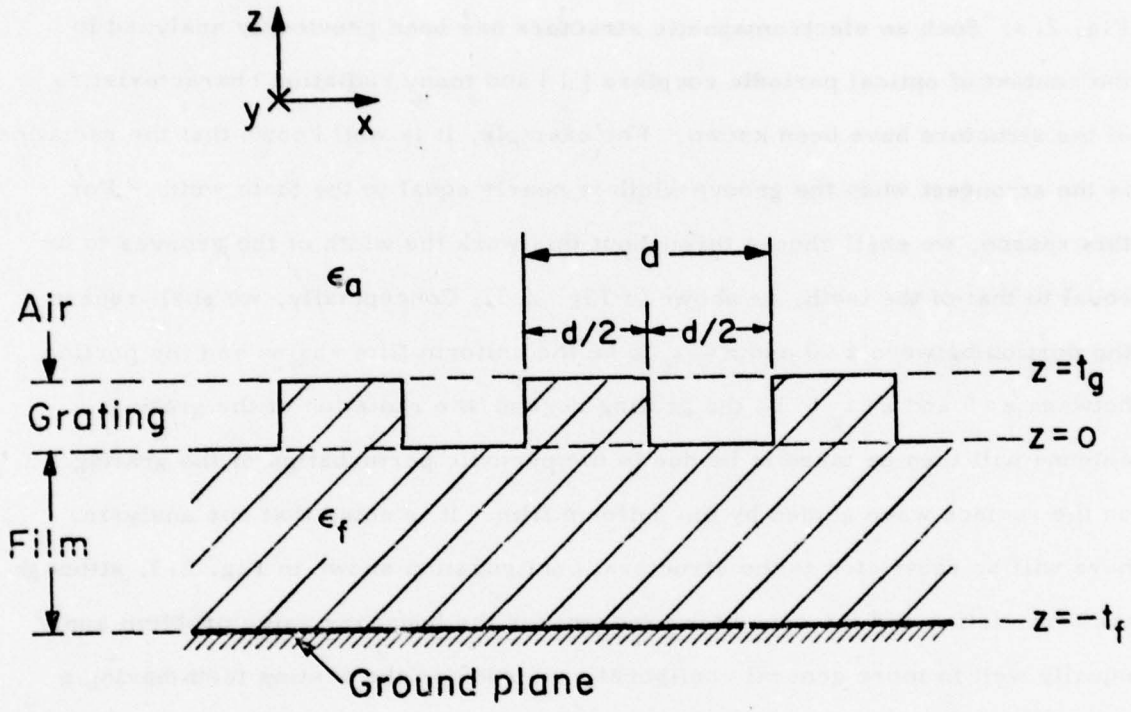

Fig. 2.3. Configuration of grating antennas.

where $\sum_n$ stands for the summation over n from $-\infty$ to ∞; for simplicity, this convention will be followed throughout this work, unless otherwise specified. I_n is the n-th harmonic amplitude of the magnetic field and k_{xn} is the x-component of the propagation constant of the n-th harmonic and is related to that of the fundamental harmonic by:

$$k_{xn} = k_{xo} + 2n\pi/d = \beta - j\alpha + 2n\pi/d = \beta_n - j\alpha \tag{2.3}$$

where β and α are the propagation and attenuation constant of the fundamental harmonic. It is noted that the propagation constant of the n-th harmonic differs from that of any other harmonic but the attenuation constant, α, is the same for all harmonics. By solving the boundary value problem, it has been shown that k_{xo} and the harmonic amplitudes, $\{I_n \mid n = 0, \pm 1, \pm 2, \cdots\}$, can be determined in terms of the eigenvalues and eigenvectors of a coupling matrix characterizing the grating. For the given antenna structure, because the energy can only radiate into the air region, it is unnecessary to determine explicitly the harmonic amplitudes, if we are interested only in the case of single beam radiation. In the present study, therefore, we are left with only the determination of dispersion root k_{xo} of the antenna. For simplicity, k_{xo} will be referred to as the leaky wave constant. Since α may be used as a measure of the rate of energy leakage, it will also be called the leakage constant, in constrast to the propagation constant β.

From Fig. 2.2, we observe that $t_f \leq 0.2\lambda$ will ensure the existence of only the fundamental mode, if the grating thickness is not unreasonably large. Also, we further observe that a larger value of t_f/λ will yield smaller change in n_{eff} in response to a change in t_f/λ. This means physically that at a high frequency, the thickness of the film does not affect appreciably the basic surface wave and the fabrication tolerance on the film thickness will not be a serious problem. On the other hand, for the frequency scanning of the radiation, (2.7) shows that λ should be chosen such that n_{eff} changes most rapidly with λ. This means that

t_f/λ should be small ($t_f/\lambda \approx 0.1$). Therefore, between the fabrication tolerance and the scanning angle, a trade-off must be imposed.

In the air region where the medium is uniform, each harmonic propagates independently as a plane wave. The transverse propagation constant of the n-th harmonic is given by:

$$k_{zn} = (k_o^2 - k_{xn}^2)^{1/2} \quad . \tag{2.4}$$

For a very thin grating or t_g very small, it is intuitively expected that $k_{xo} \approx \beta_{sw} = k_o n_{eff}$, where β_{sw} is the longitudinal propagation constant of uniform film in the absence of the grating, as shown in Fig. 2.2. Under such an approximation and invoking (2.3), we obtain, from (2.4):

$$k_{zn} = k_o[1 - (n_{eff} + n\frac{\lambda}{d})^2]^{1/2} \tag{2.5}$$

For only the n = -1 harmonic to radiate, we must have $k_{z,-1}$ *real and all* k_{zn} imaginary for $n \neq -1$. These conditions can alternatively be expressed as:

$$\frac{\lambda}{n_{eff}+1} < d < \frac{\lambda}{n_{eff}-1} \quad , \quad \text{for} \quad n_{eff} > 3 \tag{2.6a}$$

$$\frac{\lambda}{n_{eff}+1} < d < \frac{2\lambda}{n_{eff}+1} \quad , \quad \text{for} \quad n_{eff} < 3 \tag{2.6b}$$

Under these conditions, the n = -1 harmonic radiates into the air region at an angle (with respect to the z-axis):

$$\theta_{-1} = \sin^{-1}(\beta_{-1}/k_o) = \sin^{-1}(n_{eff} - \frac{\lambda}{d}) \tag{2.7}$$

The sign of θ_{-1} determines the forward or backward radiation. Although the above design formulas are derived under the assumption that t_g is very small, they also hold for t_g large, except that the value of n_{eff} has to be corrected due to the perturbation of the grating. For most practical cases where t_g is not very large, n_{eff} of the basic surface wave should give a fairly accurate estimate of the range of d and the angle of radiating beam for preliminary design considerations.

1. Effect of the Periodicity

While the principle of grating antennas is based on the periodic nature of the structure, it is expected that the periodicity of the grating plays the most important role in the operation of this class of antennas. For a trial calculation, we choose the parameters: $t_f = 0.2\lambda$ and $t_g = 0.05\lambda$, which ensure the existence of only the fundamental mode for all three materials under consideration. The leaky wave constant as a function of the periodicity is plotted in Figs. 2.4 for $\varepsilon_f = 12$. Figure 2.4(a) is a partial Brillouin diagram for the periodic structure. It is noted that the curve is interrupted in the vicinity of $\beta d/2\pi = 1.0$. This is a region of strong interaction between the fundamental and the second harmonic to produce a stopband. In the vicinity of the stopband, we have encountered numerical difficulties in dealing with multi-valued functions of the dispersion relation for the periodic medium. Such difficulties remain to be overcome.

Figure 2.4(b) shows the leakage constant for a range of d where a single beam radiates, with some angles of radiation indicated. We observe that for the parameters chosen and with $\varepsilon_f = 12$, the leakge constant is large enough (over a large range of d/λ) for the grating antenna to be useful for mm-wave applications. This is the first positive result in this exploratory study. It is noted that the stopband corresponds to the broadside radiation which covers about an angle of 15°. The detailed characteristics of broadside radiation remains to be investigated.

The same analysis has also been carried out for $\varepsilon_f = 10$ and 4 and the results are plotted in Figs. 2.5 and 2.6. Although the $\alpha\lambda$ value calculated is relatively low for the case $\varepsilon_f = 10$, it can be increased by changing some of the structural parameters, such as t_g, as will be tried next. For the case $\varepsilon_f = 4$, however, the $\alpha\lambda$ value is too small over almost the entire range of d and it does not seem to be useful for mm-wave antenna applications.

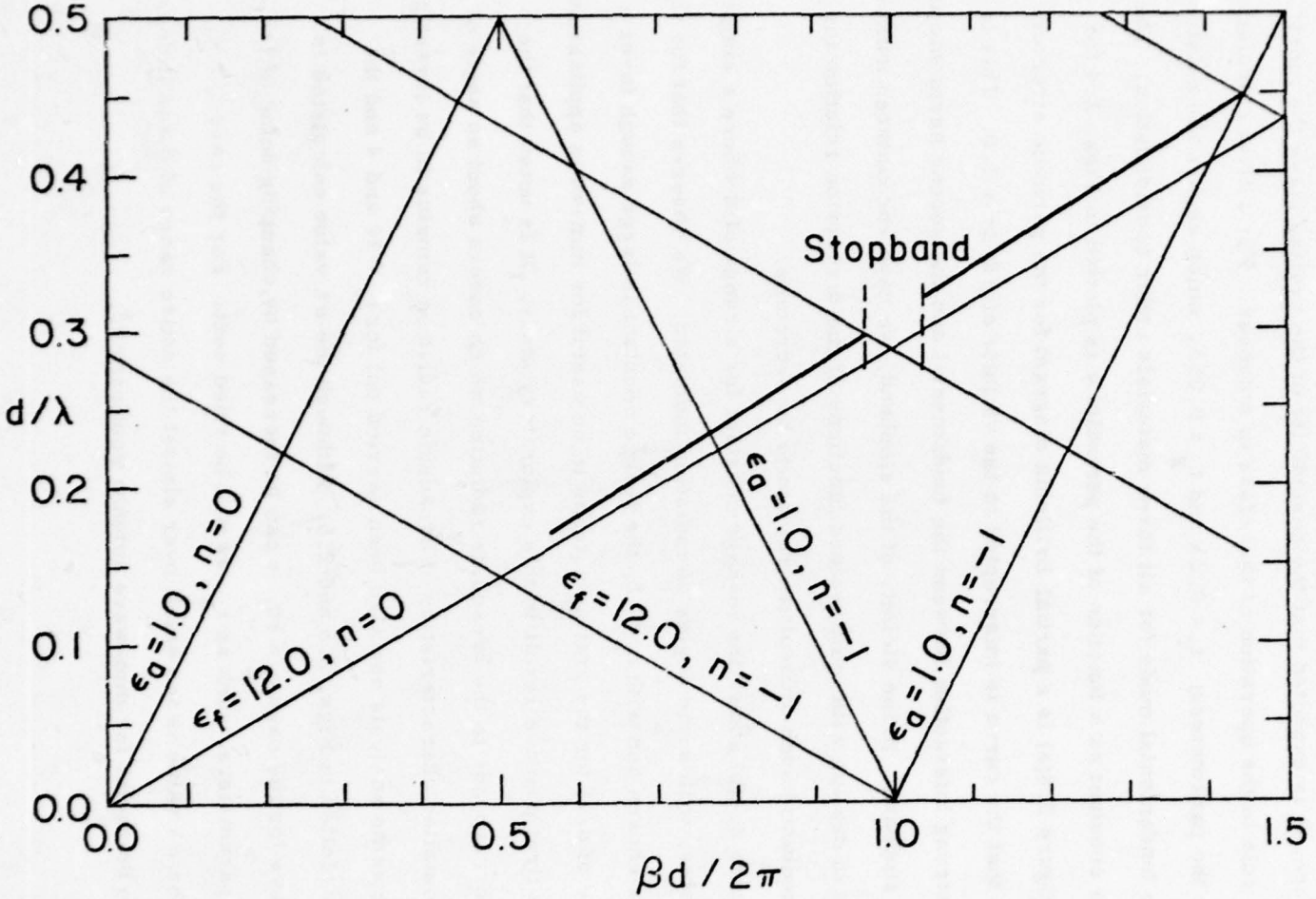

Fig. 2.4(a). Dispersion curves for silicon grating antenna - propagation constant.

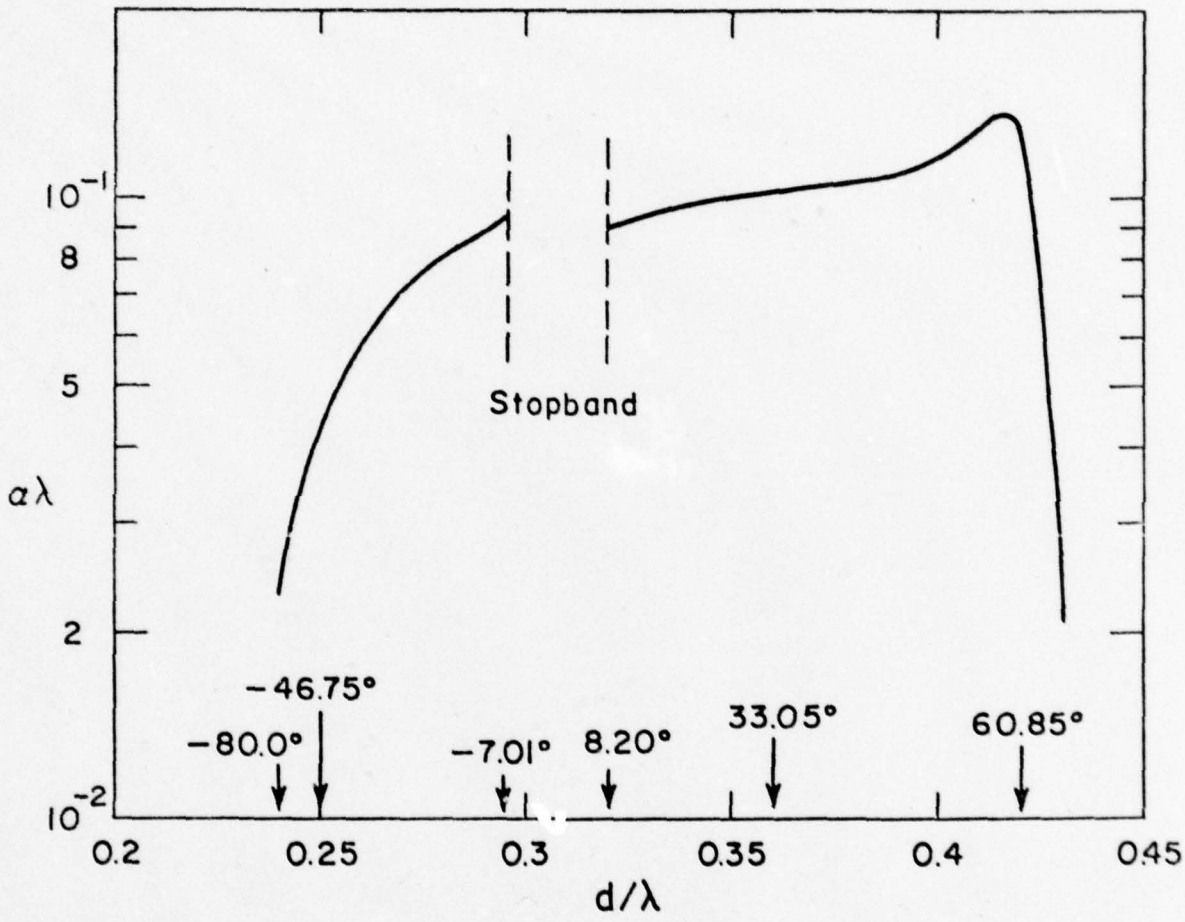

Fig. 2.4(b). Dispersion curves for silicon grating antenna - leakage constant.

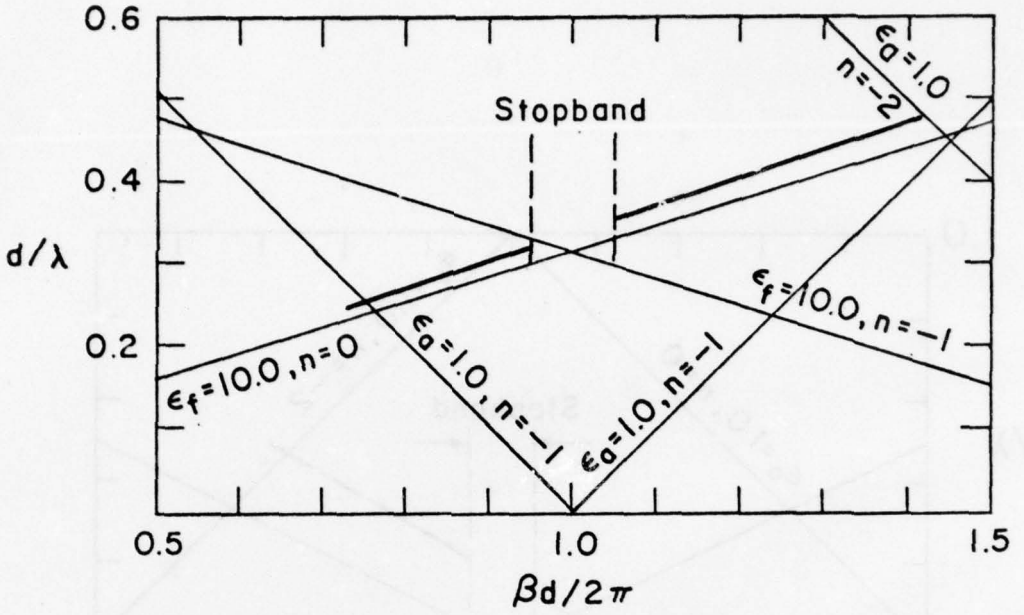

(a) Propagation constant

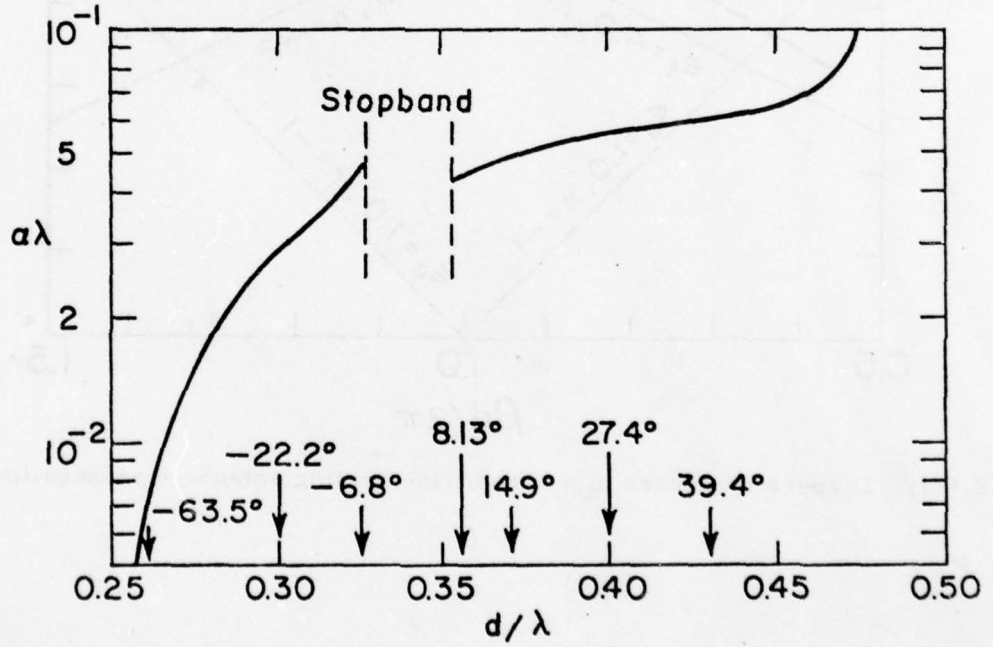

(b) Leakage constant

Fig. 2.5. Dispersion curves for Al_2O_3 grating antenna.

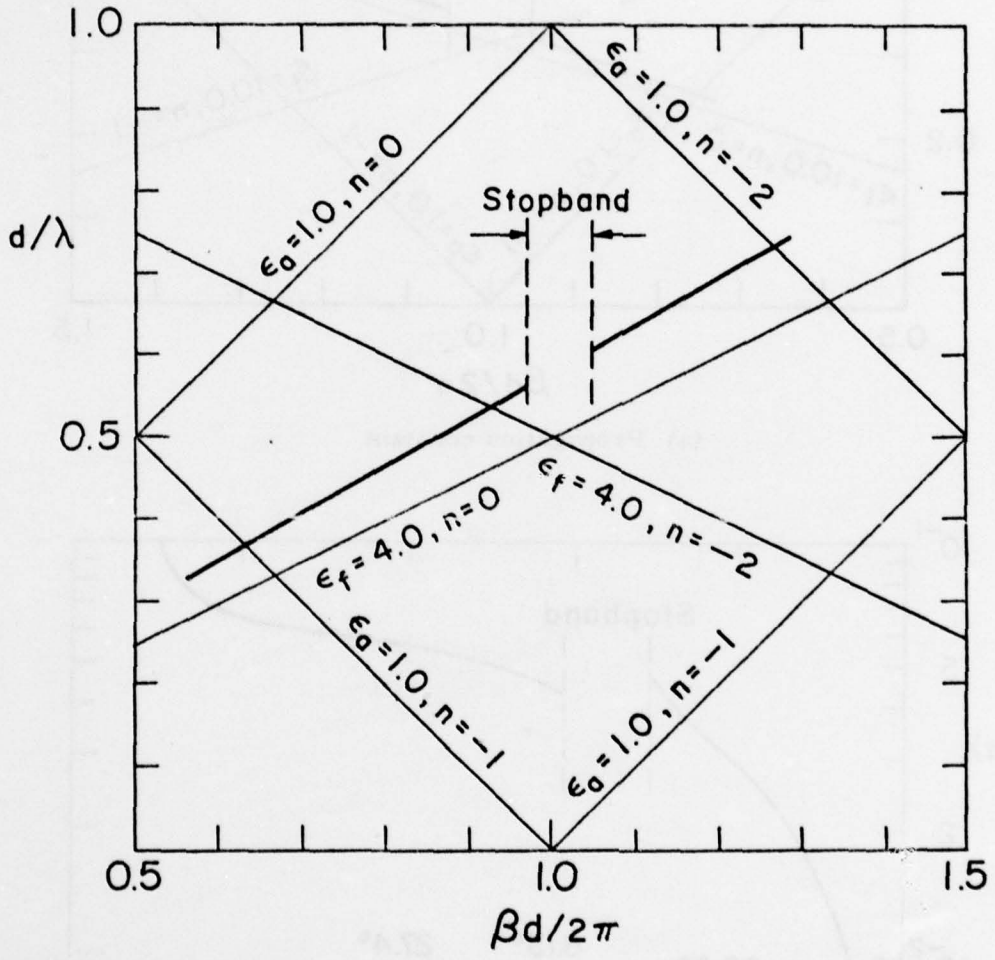

Fig. 2.6(a). Dispersion curves of a boronitride grating antenna - propagation constant.

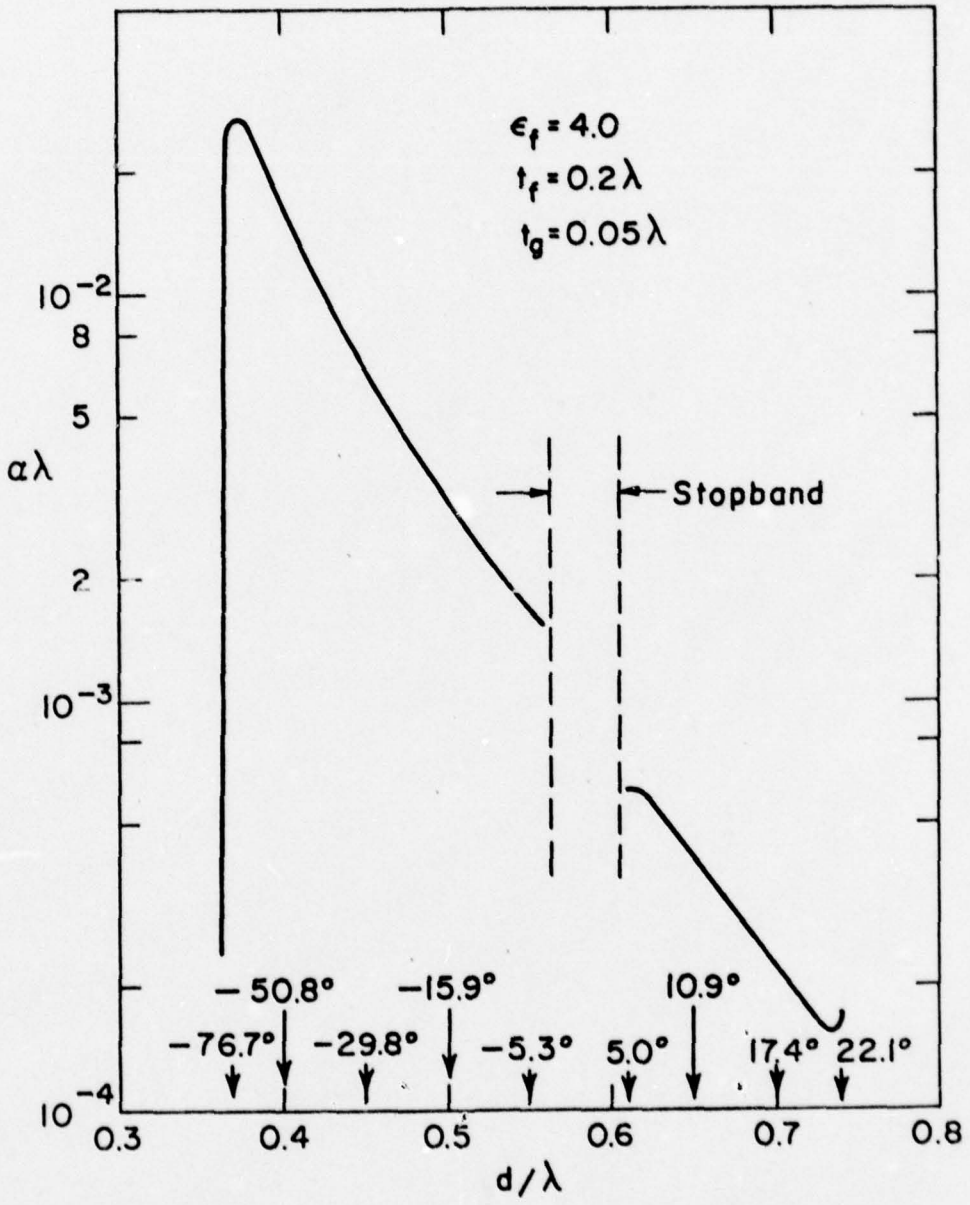

Fig. 2.6(b). Dispersion curves for boronitride grating antenna -- leakage constant.

2. Effect of Grating Thickness

Referring to Figs. 2.4, 2.5 and 2.6, we find that the $\alpha\lambda$ value is relatively low for the backward radiation. It is hoped that by increasing the grating thickness, $\alpha\lambda$ may be increased substantially so that the backward radiation may also be utilized for mm-wave antenna systems. An appropriate value of d is chosen for each value of ϵ_f and the leakage constant as a function of t_g/λ is plotted in Fig. 2.7. $\alpha\lambda$ is proportional to t_g^2, for t_g small and reaches a saturation value, for t_g large, as expected. For $\epsilon_f = 10$ and 12, $\alpha\lambda$ can indeed be increased to a large value by increasing t_g; hence, the backward radiation can be utilized. For $\epsilon_f = 4.0$, however, $\alpha\lambda$ is still too low for a large range of t_g and, again, does not seem to be of any practical interest for mm-wave antenna applications.

3. Frequency Scanning of a Radiating Beam

The scanning of a radiating beam has been an important problem in antenna applications; especially, the scanning by an electronic mean has been in great demand. One important characteristic of a periodic antenna is that the radiating beam can be scanned electronically by changing the frequency (or equivalently the wavelength) of an excitation source. Unfortunately, accompanying the beam scanning, other effects may also arise due to the change in frequency. For s sufficiently long antenna which is implicitly assumed throughout this work, the most important effect is the variation of the beam width during the scanning process. Since the beam width depends solely on the leakage constant α, we determine here the leakage constant along with the radiation angle as a function of the wavelength, with all other structural parameters being kept constant.

Figure 2.8 shows scanning characteristics of a silicon grating antenna, for two values of periodicity length: d = 1.05 mm for the forward radiation and d = 0.81 mm for the backward radiation. In both cases, $\alpha\lambda$ reaches a peak value near λ = 3 mm and decreases almost symmetrically from the peak value as the wavelength changes. On the other hand, the radiation angle varies almost linearly

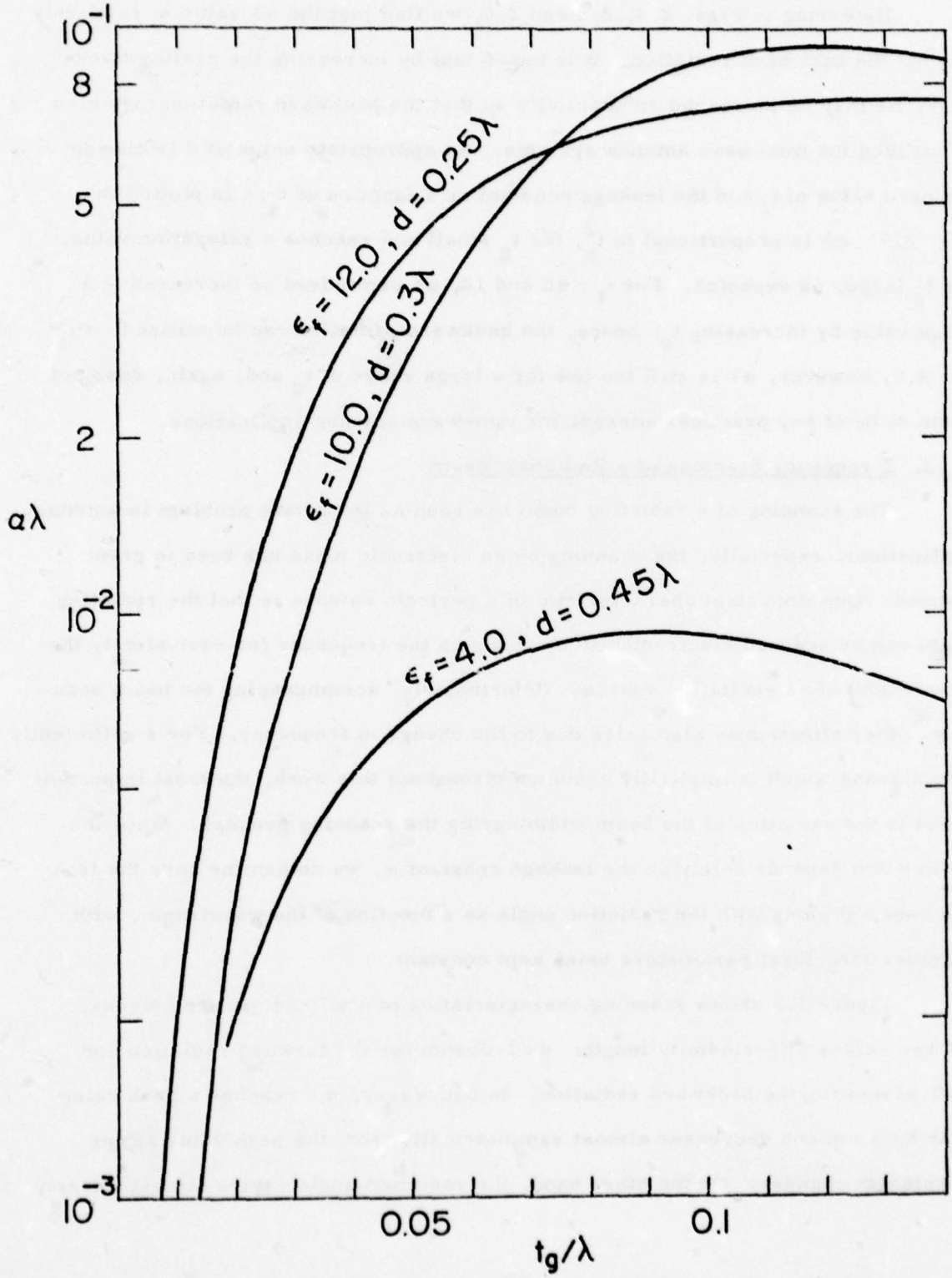

Fig. 2.7. Effect of grating thickness on leakage constant.

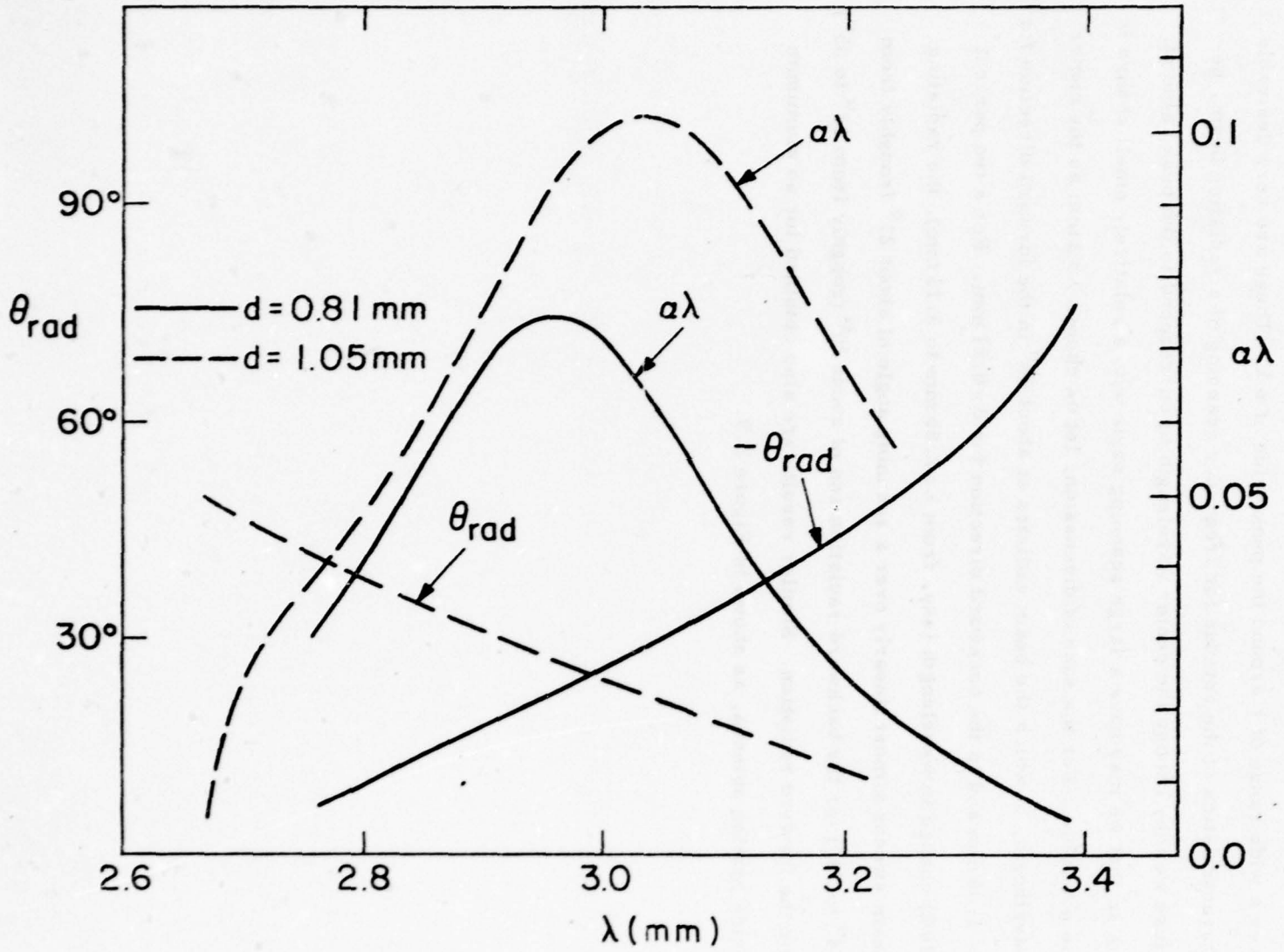

Fig. 2.8. Frequency scanning characteristics of a silicon grating antenna.

over a wide range of λ around the peak value of $\alpha\lambda$. These are very desirable characteristics of the antenna for frequency scanning of a radiating beam, because we may choose the center wavelength to correspond to the peak value of $\alpha\lambda$ so that we may have a large scanning angle with a relatively small change in the $\alpha\lambda$ value. For the sake of discussion, let us choose $\lambda = 3$ mm as the center wavelength, at which the beam radiates at about 25° in the forward direction for $d = 1.05$ mm and in the backward direction for $d = 0.81$ mm. For a ten percent (10%) change in wavelength (say, from $\lambda = 2.85$ mm to 3.15 mm), the radiating beam sweeps almost linearly over a scanning angle of about 25° (roughly from 14° to 39°) for the backward radiation and of about 20° (roughly from 15° to 35°) for the forward radiation. Similar results are also obtained for an aluminum oxide grating antenna, as shown in Figure 2.9.

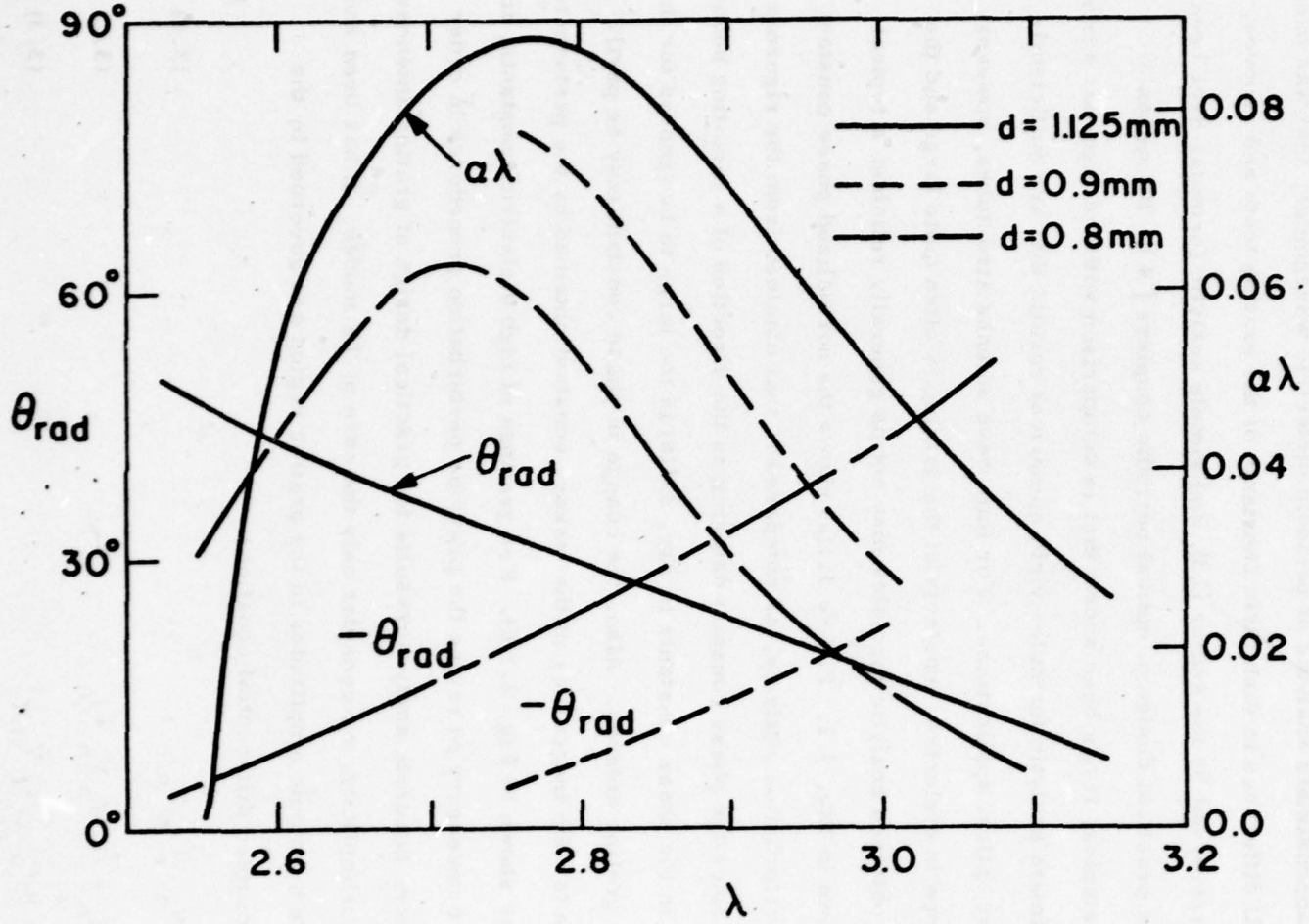

Fig. 2.9. Frequency scanning characteristics of an aluminum oxide grating antenna. $t_f = 0.6$ mm and $t_g = 0.15$ mm.

III. APPROXIMATE ANALYSIS

An approximate analysis of periodic dielectric waveguides, that was based on the small difference in dielectric constants of the grating teeth and grooves, has been carried out by the author [2,3], and simple analytic formulas have been obtained for practical design of optical periodic couplers [4]. By means of specific examples, it has been shown that in comparison with the rigorous analysis, the approximate analytic formulas yield numerical results that are sufficiently accurate for optical applications. For mm-wave antenna structures, however, the difference in dielectric constants of the grating is often quite large and the previously obtained analytic formulas may not be generally reliable: a typical case is shown in Fig. 3.1. Figure 3.1(a) shows the normalized phase constant used in a perturbation analysis, as compared to that obtained from the rigorous analysis. Since the phase constant determines the direction of a radiating beam, the change in the phase constants in Fig. 3.1(a) is too large to be ignored for the design of a grating antenna. Also, the change in phase constant may be partly responsible for the inaccuracy of the leakage constant obtained by the perturbation analysis, as shown in Fig. 3.1(b). For gratings of high dielectric constants, it is therefore necessary to revise the previous perturbation procedures in order to obtain more accurate analytic results for practical design of grating antennas.

For simplicity, we consider only the case of TE modes. It has been shown [1] that the harmonic amplitudes in the grating region are governed by the system of coupled differential equations:

$$\frac{d}{dz} V_n = i \kappa_n Z_n I_n \tag{3.1}$$

$$\frac{d}{dz} I_n = i \kappa_n Y_n V_n + j_n \tag{3.2}$$

$$j_n = i\omega\epsilon_o \sum_{\ell \neq 0} \epsilon_\ell V_{n-\ell} \tag{3.3}$$

for every $n = 0, \pm 1, \pm 2, \cdots$ and where j_n represents the coupling terms, due to the

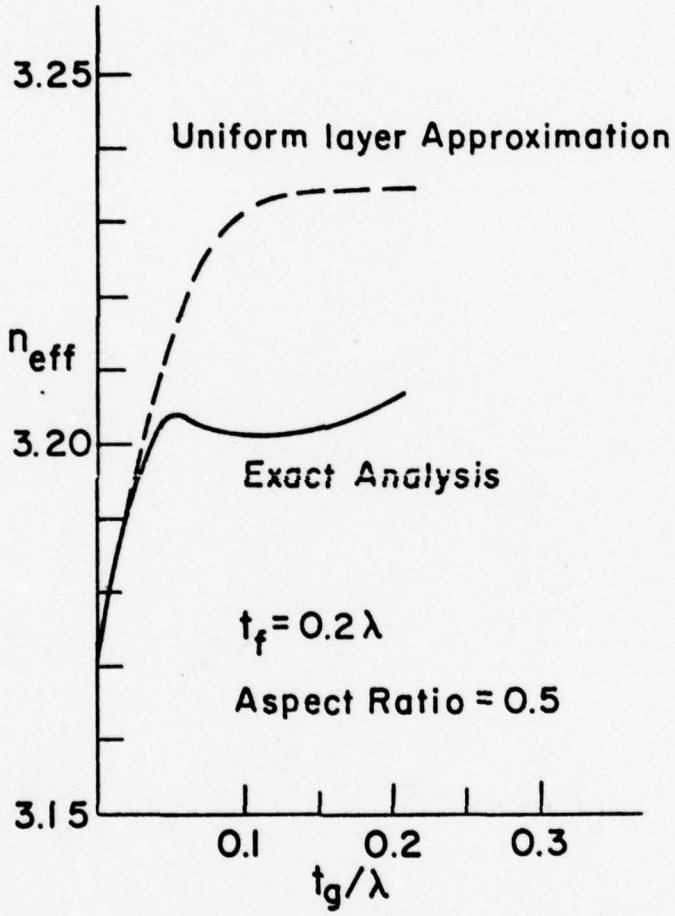

Fig. 3.1(a). Effect of grating thickness on the effective index of refraction for a silicon grating antenna - a comparison between the exact and the perturbation analysis.

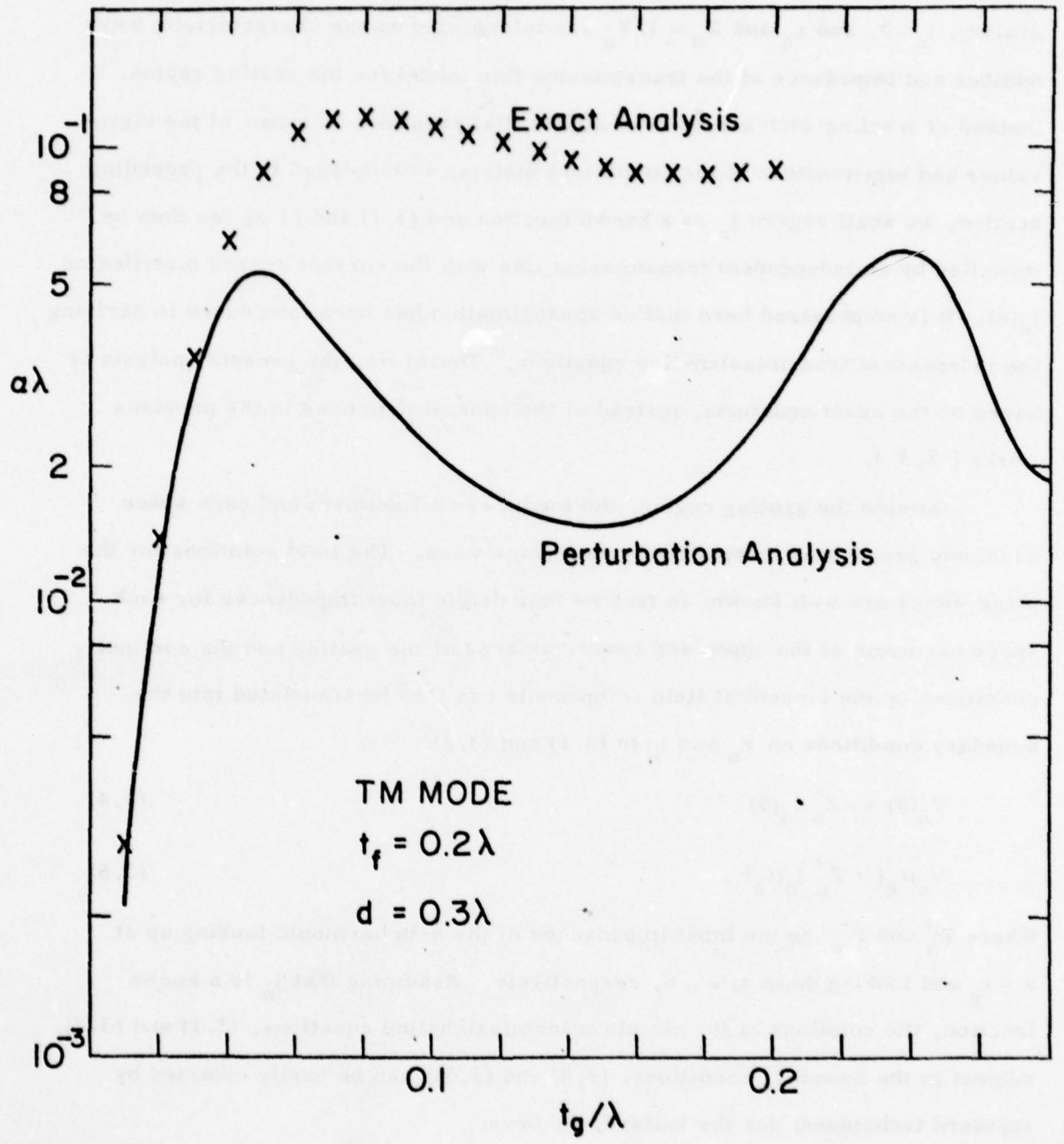

Fig. 3.1(b). Effect of grating thickness on the leakage constant for a silicon grating antenna - a comparison between the exact and the perturbation analysis.

periodic variation of the grating. In the absence of the periodic variation of the grating, $j_n = 0$, and κ_n and $Z_n = 1/Y_n$ are interpreted as the characteristic wave number and impedance of the transmission line model for the grating region. Instead of treating such a system of differential equations in terms of the eigenvalues and eigenvectors of the coefficient matrix, as employed in the preceding section, we shall regard j_n as a known function and (3.1) and (3.2) can then be modelled by an independent transmission line with the current source distribution $j_n(z)$. It is emphasized here that no approximation has been introduced in deriving the independent transmission-line equations. Therefore, the present analysis is based on the exact equations, instead of the approximate ones in the previous works [2, 3].

Outside the grating region, the media are all uniform and each space harmonic propagates independently as a plane wave. The field solutions for the plane waves are well known; in fact we may define input impedances for each space harmonic at the upper and lower surfaces of the grating and the continuity conditions on the tangential field components can then be translated into the boundary conditions on V_n and I_n in (3.1) and (3.2):

$$V_n(0) = -Z_n^- I_n(0) \tag{3.4}$$

$$V_n(t_g) = Z_n^+ I_n(t_g) \tag{3.5}$$

where Z_n^+ and Z_n^- are the input impedances of the n-th harmonic looking up at $z = t_g$ and looking down at $z = 0$, respectively. Assuming that j_n is a known function, the solutions of the simple transmission-line equations, (3.1) and (3.2), subject to the boundary conditions, (3.4) and (3.5), can be easily obtained by standard techniques; for the voltage, we have:

$$R_n V_n(z) = \frac{1}{2} Z_n \int_0^{t_g} G_n(z, z') j_n(z') dz' \tag{3.6}$$

for every n and where R_n and G_n are defined by:

$$R_n = 1 - \gamma_n^+ \gamma_n^- \exp(i 2 \kappa_n t_g) \tag{3.7}$$

$$G_n(z, z') = \gamma_n^-[\gamma_n^+ \exp(-i \kappa_n z') + \exp(i \kappa_n z')] \exp(i \kappa_n z)$$

$$+ \gamma_n^+[\exp(-i \kappa_n z') + \gamma_n^- \exp(i \kappa_n z')] \exp(i 2 \kappa_n t_g) \exp(-i \kappa_n z)$$

$$+ R_n \exp(i \kappa_n |z - z'|) \tag{3.8}$$

in which γ_n^+ and γ_n^- are the reflection coefficients looking up at $z = t_g$ and looking down at $z = 0$, respectively; they are related to the input impedances by:

$$\gamma_n^{\pm} = (Z_n^{\pm} - Z_n)/(Z_n^{\pm} + Z_n) \quad . \tag{3.9}$$

If needed, the current I_n can then be obtained by substituting (3.6) into (3.1).

With j_n given by (3.3), however, (3.6) is actually a system of coupled integral equations from which the set V_n is still to be determined. Nevertheless, (3.6) is in a form that is convenient for applying the iteration technique, so that V_n can be determined simply and systematically to any desired degree of accuracy. In the extreme case that the periodic variation in the grating disappears, $j_n = 0$ and we must have, from (3.6), for $n = 0$:

$$R_0 = 1 - \gamma_0^+ \gamma_0^- \exp(i 2 \kappa_0 t_g) = 0 \tag{3.10}$$

which is recognized as the dispersion relation for a uniform surface waveguide. In the presence of a periodic variation, (3.6) for $n = 0$ may be recast, after performing a scalar multiplication by $V_0(z)$, into the form:

$$R_0 = \frac{1}{2} \langle V_0 | G_0 | \sum_{n \neq 0} \varepsilon_{-n} V_n \rangle / \langle V_0 | V_0 \rangle \tag{3.11}$$

in which we have made use of the notations:

$$\langle V | G | U \rangle = \int_0^{t_g} \int_0^{t_g} V^*(z) G(z, z') U(z') \, dz dz' \tag{3.11a}$$

$$\langle V | U \rangle = \int_0^{t_g} V^*(z) U(z) \, dz \quad . \tag{3.11b}$$

In comparison with (3.10), it is evident that the term on the right hand side of the equality in (3.11) represents the perturbation due to the periodic variation of the grating on the surface wave of the uniform waveguide. Equation (3.11) is an exact dispersion relation for the periodic waveguide. In this approach, the effect of the periodic perturbation is included in the dispersion relation which will automatically yield appropriate changes in both real and imaginary parts of the dispersion roots. Furthermore, the perturbation term in (3.11) is evidently a variational expression in which a first order approximation in the V's will give rise to only a second order effect in the ratio. That is, a fairly accurate estimate of the V's should yield a practically acceptable dispersion root. Therefore, the present approach is particularly simple for the first order estimate of the leaky wave constant of a grating antenna.

IV. RADIATION CHARACTERISTICS OF UNBOUNDED GRATING ANTENNAS -- -- OBLIQUE INCIDENCE

The practical problem with which we are concerned here is depicted in Fig. 4.1, in which a grating antenna is excited by a surface wave which is guided by a uniform layer in junction with the antenna at $x = 0$. In the past, the problem has been analyzed only for the special case of normal incidence (e.g., $\theta = 0$ in Fig. 4.1). In such a special case, the fields have no variation along the y-direction and we thus have a two dimensional boundary value problem of a periodic dielectric waveguide in which the TE and TM modes can be treated independently in terms of a scalar potential. When the surface wave is incident obliquely at an angle, $\theta \neq 0$, the periodic waveguide structure becomes a three dimensional boundary value problem which requires the simultaneous presence of both TE and TM modes, as previously defined [1], to satisfy the continuity conditions on all the tangential components of the electromagnetic fields, as will be shown later. In other words, TE and TM modes are generally coupled in the case of oblique incidence of a surface wave. In this section, we present an exact formulation of the three dimensional boundary value problem, properly taking into account the effect of coupling between the two modes. As will become self-evident later on, the most important building block in the formulation of the periodic waveguide problem is the scattering of plane waves by a grating sandwiched between two different uniform media. Also, such a scattering problem is of great interest in its own right. Therefore, the scattering of plane waves by a grating will be studied first and the guiding of waves by a periodic waveguide will then follow.

A. Scattering of a Plane Wave by a Periodic Layer

Consider now the scattering of a plane wave by a periodic layer, $\varepsilon(x)$, that is sandwiched between two uniform semi-infinite media. To be consistent with the waveguide problem, the upper half space is designated as the air region with the relative dielectric constant ε_a and the lower half space as the film region with

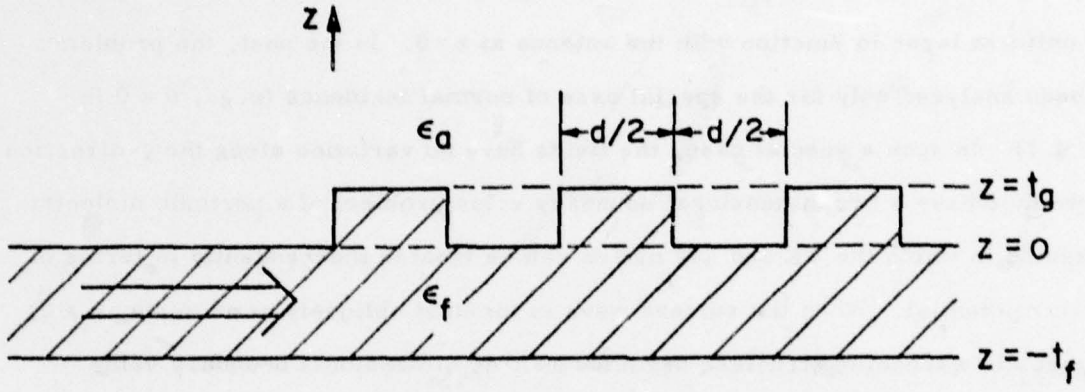

(a) Side view

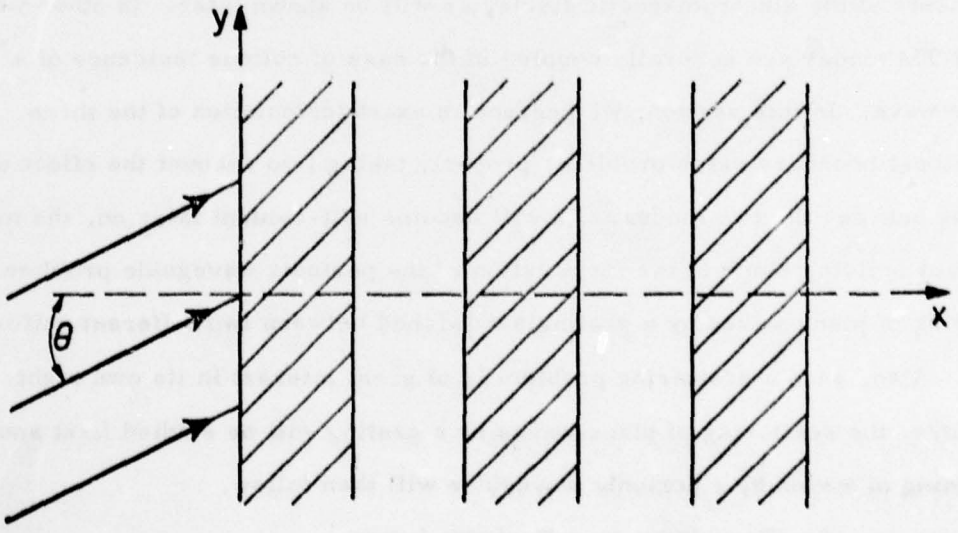

(b) Top view

Fig. 4.1. Cblique excitation of a grating antenna by a surface wave.

the dielectric constant ϵ_f. The direction of the plane wave is specified by the two angles: θ_{inc} with respect to the z-axis and ϕ_{inc} with respect to the x-axis, as shown in Fig. 4.2. The components of the propagation vector of the incident wave are:

$$k_{xo} = k_f \sin\theta_{inc} \cos\phi_{inc} \tag{4.1}$$

$$k_{yo} = k_f \sin\theta_{inc} \sin\phi_{inc} \tag{4.2}$$

$$k_{zo}^{(f)} = k_f \cos\theta_{inc} \tag{4.3}$$

$$k_f = k_o\sqrt{\epsilon_f} \tag{4.4}$$

where k_o and k_f are the plane wave propagation constants in the free space and the film region, respectively. It is noted that in the present boundary value problem, the x- and y-component of the propagation constants must be the same everywhere, but not the z-component. Therefore, it is necessary to have the superscript f to denote the region of definition for the z-component.

Due to the spatial periodicity (of the grating) in x, all the space harmonics (Fourier components) are generally excited everywhere in the structure; the propagation constant of the n-th harmonic is related to that of the incident wave by:

$$k_{xn} = k_{xo} + 2n\pi/d \quad , \quad \text{for} \quad n = 0, \pm 1, \pm 2, \cdots \tag{4.5}$$

where d is the periodicity of the grating. In particular, in the film and air regions where the media are spatially uniform, each space harmonic propagates independently as a plane wave. Although the amplitude of each plane wave remains to be determined, the propagation characteristics of each plane wave can readily be investigated through the dispersion relation, for the TE and TM modes:

$$k_{zn}^{(q)} = (k_o^2\epsilon_q - k_{yo}^2 - k_{xn}^2)^{1/2} \tag{4.6}$$

where q may stand for either f or a designating the film or air region. It is noted that the sign of the square root has to be chosen such that the radiation condition at infinity is satisfied. In the boundary value problem of plane wave scattering,

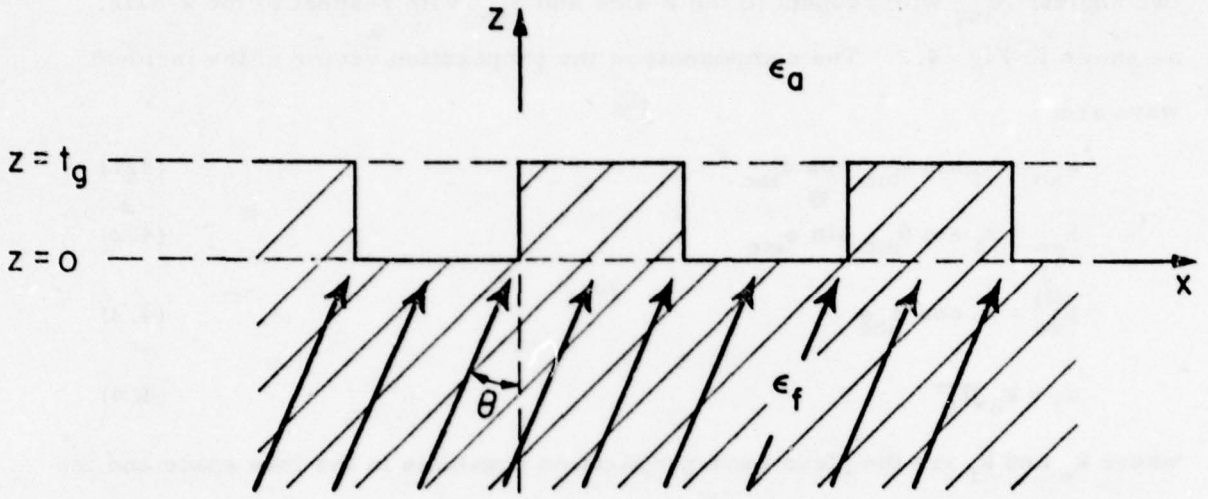

(a) Side view

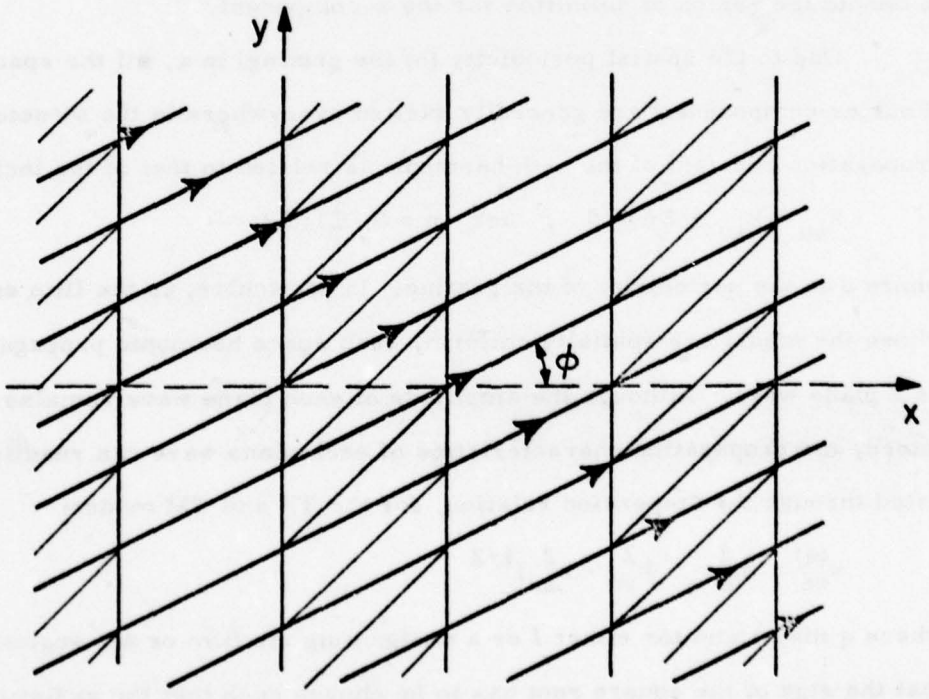

(b) Top view

Fig. 4.2. Scattering of a plane wave by a grating.

k_{yo} and k_{xo} are both real and ϵ_f and ϵ_a are both assumed real for lossless media. As a consequence, $k_{zn}^{(q)}$ is either real or imaginary, depending on n. If $k_{zn}^{(q)}$ is real, the n-th harmonic is said to be propagating transversely (along z) in the q-th medium. Otherwise, it is evanescent. From (4.5) and (4.6), it is straightforward to show that only a finite number of harmonics can propagate transversely in the air and film regions. For a propagating harmonic, the direction of propagation in the q-th medium is specified by the two angles:

$$\theta_n^{(q)} = \cos^{-1}(k_{zn}^{(q)}/k_p) \tag{4.7}$$

$$\phi_n = \tan^{-1}(k_{yo}/k_{xn}) \tag{4.8}$$

with respect to the z- and x-axis, respectively. In (4.7), k_q is the plane wave propagation constant in the q-th medium defined by

$$k_q = k_o\sqrt{\epsilon_q} \tag{4.9}$$

which generalizes (4.4). It is noted that in contrast $\theta_n^{(q)}$, ϕ_n is independent of the property of the medium in which the plane wave propagates.

The key to the present boundary value problem is the determination of a complete set of characteristic solutions of the grating region that are applicable to a given type of source excitation. We have observed that by a simple coordinate transformation, the characteristic solutions previously determined for the special case of normal incidence (of a surface wave) can also be utilized for the general case of oblique incidence. Such an observation enables us to attack with relative ease the difficult problem being analyzed here.

The characteristic solutions for the grating region have been extensively analyzed for many profiles of the periodic dielectric constant [1]. The general form of the characteristic solutions are given in Table 4.1 where k_t is the transverse propagation constant (with respect to the direction of periodic variation). It is noted that V(x) is the potential function for TE modes and I(x) for TM

TABLE 4.1. Components of characteristic field solutions in an unbounded periodic medium.

TE mode	TM mode
$E_u = \exp(i k_t v)\, V(x)$	$H_u = \exp(i k_t v)\, I(x)$
$H_x = -(k_t/\omega\mu)\, E_u$	$E_x = [k_t/\omega\varepsilon_o \varepsilon(x)]\, H_u$
$H_v = \exp(i k_t v)\, I(x)$	$E_v = \exp(i k_t v)\, V(x)$
$I(x) = -i(1/\omega\mu) \frac{d}{dx} V(x)$	$V(x) = i[1/\omega\varepsilon_o \varepsilon(x)] \frac{d}{dx} I(x)$

modes. In general, these potential functions can be represented by the Fourier series (Floquet's solutions), as shown in Table 4.2, along with other associated

TABLE 4.2. Fourier representations for transmission-line voltage and current and their related quantities.

TE mode	TM modes
$V(x) = \sum' V_n e^{i k_{xn} x}$	$[k_t/\omega\varepsilon_o \varepsilon]\, I(x) = \sum' V_n e^{i k_{xn} x}$
$(k_t/\omega\mu)\, V(x) = \sum' I_n e^{i k_{xn} x}$	$I(x) = \sum' I_n \exp(i k_{xn} x)$
$I(x) = \sum' G_n e^{i k_{xn} x}$	$V(x) = \sum' G_n \exp(i k_{xn} x)$

functions. Evidently, these characteristic solutions are invariant along the u-direction and propagate along the v-direction. The uv-coordinate system in which the TE and TM modes exist independently is shown in Fig. 4.3, with respect to the yz-coordinate system in which the structure is described. For simplicity, the former will be called the characteristic coordinate system and the latter the structural coordinate system. The transformation (rotation) between the two coordinate systems is governed by:

$$u = y \cos\psi - z \sin\psi$$
$$v = y \sin\psi + z \cos\psi \qquad (4.9)$$

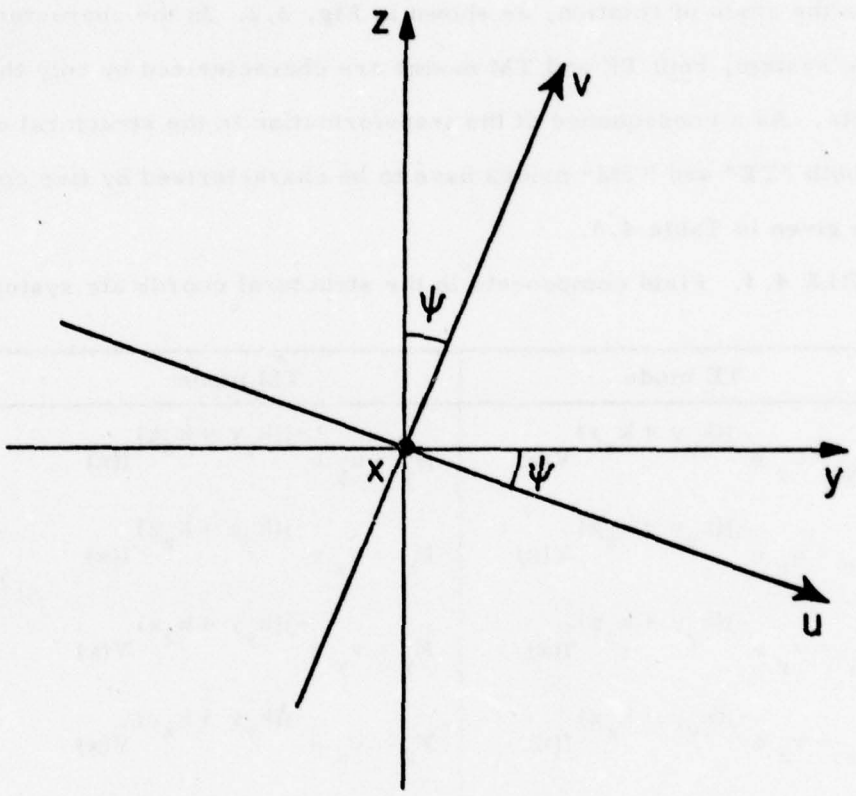

Fig. 4.3. Rotation of coordinate system around the x-axis.

or in terms of unit vectors:

$$\underline{u}_o = u_y \underline{y}_o + u_z \underline{z}_o = \underline{y}_o \cos\psi - \underline{z}_o \sin\psi$$
$$\underline{v}_o = v_y \underline{y}_o + v_z \underline{z}_o = \underline{y}_o \sin\psi + \underline{z}_o \cos\psi \qquad (4.10)$$

where ψ is the angle of rotation, as shown in Fig. 3.2. In the characteristic coordinate system, both TE and TM modes are characterized by only three field components. As a consequence of the transformation to the structural coordinate system, both "TE" and "TM" modes have to be characterized by five components which are given in Table 4.3.

TABLE 4.3. Field components in the structural coordinate system.

TE mode	TM mode
$E_y = u_y e^{-j(k_y y + k_z z)} V(x)$	$H_y = u_y e^{-j(k_y y + k_z z)} I(x)$
$E_z = u_z e^{-j(k_y y + k_z z)} V(x)$	$H_z = u_z e^{-j(k_y y + k_z z)} I(x)$
$H_y = v_y e^{-j(k_y y + k_z z)} I(x)$	$E_y = v_y e^{-j(k_y y + k_z z)} V(x)$
$H_z = v_z e^{-j(k_y y + k_z z)} I(x)$	$E_z = v_z e^{-j(k_y y + k_z z)} V(x)$
$H_x = -\frac{k_t}{\omega\mu} e^{-j(k_y y + k_z z)} V(x)$	$E_x = \frac{k_t}{\omega \varepsilon_o \varepsilon(x)} e^{-j(k_y y + k_z z)} I(x)$

For a given longitudinal propagation constant, k_{xo}, the complete set of transverse propagation constants and their corresponding Floquet solutions for the periodic medium have been previously determined for both TE and TM modes [1]. While the dispersion relations are identical for TE and TM modes in a uniform region, as given in (4.6), they are generally different for the two modes in the grating region. Therefore, we have two different sets of transverse propagation constants and Floquet solutions for the grating regions as

formally given in Table 4.4. Here, we have made use of the fact that the propagation constant k_{yo} is continuous everywhere and the propagations constant in the z-direction is determined by:

$$k'_{zm} = [(k'_{tm})^2 - k_{yo}^2]^{1/2} \quad , \quad \text{for TE modes} \tag{4.11}$$

$$k''_{zm} = [(k''_{tm})^2 - k_{yo}^2]^{1/2} \quad , \quad \text{for TM modes} \tag{4.12}$$

It is noted that k'_{zm} and k''_{zm} can only be either real or imaginary for a lossless grating. This means physically that the mode can be either propagating or evanescent if the grating is lossless.

Referring to Fig. 4.2(a), since the plane wave is incident in the forward direction from the film region, the reflected waves consist of all the space harmonics propagating in the backward direction. With the y-dependence, $\exp(ik_{yo}y)$, understood and suppressed for simplicity, the tangential components of the field solutions in the film region, $z < 0$, can be written as:

$$E_x^{(f)}(x,z) = \sum_n [k_{tn}^{(f)}/\omega\varepsilon_o\varepsilon_f][a''_o\delta_{no}\exp(ik_{zo}^{(f)}z) + b''_n\exp(-ik_{zn}^{(f)}z)]\exp(ik_{xn}x) \tag{4.13a}$$

$$E_y^{(f)}(x,z) = \sum_n u_{yn}^{(f)}[a'_o\delta_{no}\exp(ik_{zo}^{(f)}z) + b'_n\exp(-ik_{zn}^{(f)}z)]\exp(ik_{xn}x) \tag{4.13b}$$

$$- \sum_n v_{yn}^{(f)}[k_{xn}/\omega\varepsilon_o\varepsilon_f][a''_o\delta_{no}\exp(ik_{zo}^{(f)}z) + b''_n\exp(ik_{zn}^{(f)}z)]\exp(ik_{xn}x)$$

$$H_x^{(f)}(x,z) = -\sum_n [k_{tn}^{(f)}/\omega\mu][a'_o\delta_{no}\exp(ik_{zo}^{(f)}z) - b'_n\exp(-ik_{zn}^{(f)}z)]\exp(ik_{xn}x) \tag{4.13c}$$

$$H_y^{(f)}(x,z) = \sum_n v_{yn}^{(f)}[k_{xn}/\omega\mu][a'_o\delta_{no}\exp(ik_{zo}^{(f)}z) - b'_n\exp(-ik_{zn}^{(f)}z)]\exp(ik_{xn}x) \tag{4.13d}$$

$$+ \sum_n u_{yn}^{(f)}[a''_o\delta_{no}\exp(ik_{zo}^{(f)}z) - b''_n\exp(-ik_{zn}^{(f)}z)]\exp(ik_{xn}x)$$

where a'_o and a''_o are, respectively, the amplitudes of the incident TE and TM waves and b'_n and b''_n are the n-th harmonic amplitudes of the reflected TE and

TABLE 4.4. Fourier series representations for tangential field components.

TE mode	TM mode
$E'_{ym} = u_{ym} e^{-jk'_{zm}z} \sum_n V'_{mn} e^{-jk_{xn}x}$	$H''_{ym} = u''_y e^{-jk''_{zm}z} \sum_n I''_{mn} e^{-jk_{xn}x}$
$H'_{xm} = -e^{-jk'_{zm}z} \sum_n I'_{mn} e^{-jk_{xn}x}$	$E''_{xm} = e^{-jk''_{zm}z} \sum_n V''_{mn} e^{-jk_{xn}x}$
$H'_{ym} = v'_{ym} e^{-jk'_{zm}z} \sum_n G'_{mn} e^{-jk_{xn}x}$	$E''_{ym} = v''_{ym} e^{-jk''_{zm}z} \sum_n G''_{mn} e^{-jk_{xn}x}$

TM waves, respectively. In the grating region bounded by the two surfaces at $z = 0$ and t_g, the electromagnetic fields consist of both forward and backward waves. From Table 4.4, the general solutions are:

$$E_x^{(g)}(x,z) = \sum_m [k''_{tm}/\omega\varepsilon_o][c''_m \exp(ik''_{zm}z) + d''_m \exp(-ik''_{zm}z)] \sum_n V''_{mn} \exp(ik_{xn}x) \tag{4.14a}$$

$$E_y^{(g)}(x,z) = \sum_m u'_{ym}[c'_m \exp(ik'_{zm}z) + d'_m \exp(-ik'_{zm}z)] \sum_n V'_{mn} \exp(ik_{xn}x)$$
$$+ \sum_m v''_{ym}[c''_m \exp(ik''_{zm}z) + d''_m \exp(-ik''_{zm}z)] \sum_n G''_{mn} \exp(ik_{xn}x) \tag{4.14b}$$

$$H_x^{(g)}(x,z) = -\sum_m [c'_m \exp(ik'_{zm}z) + d'_m \exp(-ik'_{zm}z)] \sum_n I'_{mn} \exp(ik_{xn}x) \tag{4.14c}$$

$$H_y^{(g)}(x,z) = \sum_m v'_{ym}[c'_m \exp(ik'_{zm}z) - d'_m \exp(-ik'_{zm}z)] \sum_n G'_{mn} \exp(ik_{xn}x)$$
$$+ \sum_m u''_{ym}[c''_m \exp(ik''_{zm}z) - d''_m \exp(-ik''_{zm}z)] \sum_n I''_{mn} \exp(ik_{xn}x) \tag{4.14d}$$

Here, all the quantities are known, except the mode amplitudes c's and d's. Finally, the transmitted waves in the air region, $z > t_g$, consist of only the forward waves and are given by:

$$E_x^{(a)}(x,z) = \sum_n e''_n u^{(a)}_{yn}[k^{(a)}_{tn}/\omega\varepsilon_o\varepsilon_a] \exp(ik^{(a)}_{zn}z) \exp(ik_{xn}x) \tag{4.15a}$$

$$E_y^{(a)}(x,z) = \sum_n e'_n u^{(a)}_{yn} \exp(ik^{(a)}_{zn}z) \exp(ik_{xn}x)$$
$$- \sum_n e''_n v^{(a)}_{yn}[k_{xn}/\omega\varepsilon_o\varepsilon_a] \exp(ik^{(a)}_{zn}z) \exp(ik_{xn}x) \tag{4.15b}$$

$$H_x^{(a)}(x,z) = \sum_n e'_n [k^{(a)}_{tn}/\omega\mu] \exp(ik^{(a)}_{zn}z) \exp(ik_{xn}x) \tag{4.15c}$$

$$H_y^{(a)}(x,z) = \sum_n e'_n v_{gn}[k_{xn}/\omega\mu] \exp(ik_{zn}^{(a)} z) \exp(ik_{xn} x)$$

$$+ \sum_n e''_n u_{yn}^{(a)} \exp(ik_{zn}^{(a)} z) \exp(ik_{xn} x) \tag{4.15d}$$

where e'_n and e''_n are the space harmonic amplitudes of the TE and TM waves in the air region.

To determine the scattered field amplitudes, we now match the boundary conditions at the two interfaces of the grating. The continuity of the tangential field components at $z = 0$ requires:

$$E_x^{(g)}(x,o) = E_x^{(f)}(x,o) \tag{4.16a}$$

$$E_y^{(g)}(x,o) = E_y^{(f)}(x,o) \tag{4.16b}$$

$$H_x^{(g)}(x,o) = H_x^{(f)}(x,o) \tag{4.16c}$$

$$H_y^{(g)}(x,o) = H_x^{(f)}(x,o) \tag{4.16d}$$

Substituting (4.13) and (4.14) into (4.16) and then equating the corresponding amplitudes on both sides of the equalities, we obtain the following system of equations:

$$\sum_m (k''_{tm}/\omega\varepsilon_o) V''_{mn}[c''_m + d''_m] = (k_{tn}^{(f)}/\omega\varepsilon_o\varepsilon_f)[a''_n \delta_{no} + b''_n] \tag{4.17a}$$

$$\sum_m u'_{ym} V'_{mn}[c'_m + d'_m] + \sum v''_{ym} G''_{mn}[c''_m + d''_m]$$

$$= u_{yn}^{(f)}[a'_n \delta_{no} + b'_n] - v_{yn}^{(f)}(k_{xn}/\omega\mu)[a''_n \delta_{no} + b''_n] \tag{4.17b}$$

$$\sum_m I'_{mn}[c'_m - d'_m] = (k_{tn}^{(f)}/\omega\mu)[a'_{no} \delta_{no} - b'_n] \tag{4.17c}$$

$$\sum_m v'_{ym} G'_{mn}[c'_m - d'_m] + \sum_m u''_{ym} I''_{mn}[c''_m - d''_m]$$

$$= v_{yn}^{(f)}(k_{xn}/\omega\mu)[a'_o \delta_{no} - b'_n] + u_{yn}^{(f)}[a''_o \delta_{no} - b''_n] \tag{4.17d}$$

for every $n = 0, \pm 1, \pm 2, \cdots$. Similarly, at $z = t_g$, we must have:

$$E_x^{(g)}(x, t_g) = E_x^{(a)}(x, t_g) \tag{4.18a}$$

$$E_y^{(g)}(x, t_g) = E_y^{(a)}(x, t_g) \tag{4.18b}$$

$$H_x^{(g)}(x, t_g) = H_x^{(a)}(x, t_g) \tag{4.18c}$$

$$H_y^{(g)}(x, t_g) = H_y^{(a)}(x, t_g) \tag{4.18d}$$

Substituting (4.14) and (4.15) into (4.18) and then equating the corresponding amplitudes on both sides of the equalities, we obtain the following system of equations:

$$\sum_m (k''_{tm}/\omega\varepsilon_o)\, V''_{mn} [\exp(ik''_{zm} t_g)\, c''_m + \exp(-ik''_{zm} t_g)\, d''_m] = (k_{tn}^{(a)}/\omega\varepsilon_o) \exp(ik_{zn}^{(a)} t_g)\, e''_n \tag{4.19a}$$

$$\sum_m u'_{ym} V'_{mn} [\exp(ik'_{zm} t_g)\, c'_m + \exp(-ik'_{zm} t_g)\, d'_m] + \sum_m v''_{ym} G''_{mn} [\exp(ik''_{zm} t_g)\, c''_m + \exp(-ik''_{zm} t_g)\, d''_m] = u_{yn}^{(a)} \exp(ik_{zn}^{(a)} t_g)\, e'_n - v_{yn}^{(a)} (k_{xn}/\omega\mu) \exp(ik_{zn}^{(a)} t_g)\, e''_n \tag{4.19b}$$

$$\sum_m I'_{mn} [\exp(ik'_{zm} t_g)\, c'_m - \exp(-ik'_{zm} t_g)\, d'_m] = (k_{tn}^{(a)}/\omega\mu) \exp(k_{zn}^{(a)} t_g)\, e'_n \tag{4.19c}$$

$$\sum_m v'_{ym} G'_{mn} [\exp(ik'_{zm} t_g)\, c'_m - \exp(-ik'_{zm} t_g)\, d'_m] + \sum_m u''_{ym} I''_{mn} [\exp(ik''_{zm} t_g)\, c''_m - \exp(-ik''_{zm} t_g)\, d''_m] = v_{yn}^{(a)} (k_{xn}/\omega\mu) \exp(ik_{zn}^{(a)} t_g)\, e'_n + u_{yn}^{(a)} \exp(ik_{zn}^{(a)} t_g)\, e''_n \tag{4.19d}$$

for every $n = 0, \pm 1, \pm 2, \cdots$. In the matrix form, (4.17) and (4.19) may be written succinctly as:

$$E'' K_t''[\underline{c} + \underline{d}] = \frac{1}{\varepsilon_f} K_t^{(f)} [\underline{a}'' + \underline{b}''] \tag{4.20a}$$

$$E' U_y'[\underline{c}' + \underline{d}'] + S'' V_y''[\underline{c}'' + \underline{d}''] = U_y^{(f)}[\underline{a}' + \underline{b}'] - V_y^{(f)} Y_x[\underline{a}'' + \underline{b}''] \tag{4.20b}$$

$$H'[\underline{c}' - \underline{d}'] = \frac{1}{\omega \mu} K_t^{(f)}[\underline{a}' - \underline{b}'] \tag{4.20c}$$

$$S' V_y'[\underline{c}' - \underline{d}'] + I'' U_y''[\underline{c}'' - \underline{d}''] = V_y^{(f)} Y_x[\underline{a}' - \underline{b}'] + U_y^{(f)}[\underline{a}'' - \underline{b}''] \tag{4.20d}$$

$$E'' K_t''[\exp(i K_z'' t_g)\underline{c}'' + \exp(-i K_z'' t_g)\underline{d}''] = K_t^{(a)} \exp(i K_t^{(a)} t_g)\underline{e}'' \tag{4.21a}$$

$$E' U_y'[\exp(i K_z' t_g)\underline{c}' + \exp(-i K_z'' t_g)\underline{d}'] + S'' V_y''[\exp(i K_z'' t_g)\underline{c}'' + \exp(-i K_z'' t_g)\underline{d}'']$$
$$= U_y^{(a)} \exp(i K_z^{(a)} t_g)\underline{e}' - V_y^{(a)} Y_x \exp(i K_z^{(a)} t_g)\underline{e}'' \tag{4.21b}$$

$$H'[\exp(i K_z' t_g)\underline{c}' - \exp(-i K_z' t_g)\underline{d}'] = \frac{1}{\omega \mu} K_t^{(a)} \exp(i K_z^{(a)} t_g)\underline{e}' \tag{4.21c}$$

$$S' V_y'[\exp(i K_z' t_g)\underline{c} - \exp(-i K_z' t_g)\underline{d}'] + H'' U_y''[\exp(i K_z'' t_g)\underline{c}'' - \exp(-i K_z'' t_g)\underline{d}'']$$
$$= V_y^{(a)} Y_x \exp(i K_z^{(a)} t_g)\underline{e}' + U_y^{(a)} \exp(i K_z^{(a)} t_g)\underline{e}'' \tag{4.21d}$$

in which the matrices are defined with the general elements: $E_{mn}^{(q)} = V_{nm}^{(q)}$, $H_{mn}^{(q)} = I_{nm}^{(q)}$, $S_{mn}^{(q)} = G_{nm}^{(q)}$, $(K_t^{(q)})_{mn} = k_{tm}^{(q)} \delta_{mn}$, $(U_y^{(q)})_{mn} = u_{ym}^{(q)} \delta_{mn}$, $(V_y^{(q)})_{mn} = v_{ym}^{(q)} \delta_{mn}$, $(K_z^{(q)})_{mn} = k_{zm}^{(q)} \delta_{mn}$, where the superscript may stand for either the single prime, double prime, a or f, and finally $(Y_x)_{mn} = \delta_{mn} k_{xn}/\omega \mu$. $\underline{a}'$ and $\underline{a}''$ are column vectors with the incident TE and TM mode amplitudes at the zero-th position and zero elsewhere. $\underline{b}'$ and $\underline{b}''$ are column vectors with b_n' and b_n'' as the element at the n-th position, respectively, and similarly for all other column vectors. Here, we have eight unknown column vectors to determine in terms of the given vectors $\underline{a}'$ and $\underline{a}''$ from the eight vector equations in (4.20) and (4.21).

Equations (4.20) and (4.21) may appear to be quite complicated, but we recognize that those matrices with the superscripts a and f are all diagonal and, hence, the solutions of (4.20) and (4.21) can be obtained with relative ease. Substituting $\underline{e}'$ in (4.21c) and $\underline{e}''$ in (4.21a) into (4.21b) and (4.21d), we obtain the

super-matrix relation:

$$\begin{pmatrix} F_{11}^{+} & F_{12} \\ F_{21} & F_{22}^{+} \end{pmatrix}\begin{pmatrix} \exp(-iK_z' t_g) & 0 \\ 0 & \exp(-iK_z'' t_g) \end{pmatrix}\begin{pmatrix} \underline{d}' \\ \underline{d}'' \end{pmatrix} = \begin{pmatrix} F_{11}^{-} & -F_{12} \\ F_{21} & F_{22}^{-} \end{pmatrix}\begin{pmatrix} \exp(iK_z' t_g) & 0 \\ 0 & \exp(iK_z'' t_g) \end{pmatrix}\begin{pmatrix} c' \\ c'' \end{pmatrix} \tag{4.22a}$$

where the F's are matrices defined by:

$$F_{11}^{\pm} = E' U_y' \pm \omega\mu [K_t^{(a)}]^{-1} U_y^{(a)} H' \tag{4.22b}$$

$$F_{12} = S'' V_y'' + [K_t^{(a)}]^{-1} V_y^{(a)} Y_x E'' K_t'' \tag{4.22c}$$

$$F_{21} = S' V_y' - \omega\mu [K_t^{(a)}]^{-1} V_y^{(a)} Y_x H' \tag{4.22d}$$

$$F_{22}^{\pm} = H'' U'' \quad K_t^{(a)}]^{-1} U_y^{(a)} E'' K_t'' \tag{4.22e}$$

Furthermore, from (4.22a), we obtain:

$$\begin{pmatrix} d' \\ d'' \end{pmatrix} = \begin{pmatrix} \Gamma_{11} & \Gamma_{12} \\ \Gamma_{21} & \Gamma_{22} \end{pmatrix}\begin{pmatrix} \underline{c}' \\ \underline{c}'' \end{pmatrix} \tag{4.23a}$$

with

$$\begin{pmatrix} \Gamma_{11} & \Gamma_{12} \\ \Gamma_{21} & \Gamma_{22} \end{pmatrix} = \begin{pmatrix} \exp(iK_z' t_g) & 0 \\ 0 & \exp(iK_z'' t_g) \end{pmatrix}\begin{pmatrix} F_{11}^{+} & F_{12} \\ F_{21} & F_{22}^{+} \end{pmatrix}^{-1}\begin{pmatrix} F_{11}^{-} & -F_{12} \\ F_{21} & F_{22}^{-} \end{pmatrix}\begin{pmatrix} \exp(iK_z' t_g) & 0 \\ 0 & \exp(iK_z'' t_g) \end{pmatrix} \tag{4.23b}$$

Alternatively, (4.20) may be rewritten in the super-matrix form as:

$$\begin{pmatrix} \omega\mu H' & 0 \\ 0 & \varepsilon_f E'' K_t'' \end{pmatrix}\begin{pmatrix} \underline{c}' \\ \underline{c}'' \end{pmatrix} + \begin{pmatrix} -H' & 0 \\ 0 & \varepsilon_f E'' K_t'' \end{pmatrix}\begin{pmatrix} \underline{d}' \\ \underline{d}'' \end{pmatrix} = K_t^{(f)}\begin{pmatrix} 1 & 0 \\ 0 & 1 \end{pmatrix}\begin{pmatrix} \underline{a}' \\ \underline{a}'' \end{pmatrix} + K_t^{(f)}\begin{pmatrix} -1 & 0 \\ 0 & 1 \end{pmatrix}\begin{pmatrix} \underline{b}' \\ \underline{b}'' \end{pmatrix} \tag{4.24a}$$

$$\begin{pmatrix} E'U_y' & S''V_y'' \\ S'V_y' & H''U_y'' \end{pmatrix}\begin{pmatrix} \underline{c}' \\ \underline{c}'' \end{pmatrix} + \begin{pmatrix} E'V_y' & S''V_y'' \\ -S'V_y' & -H''U_y'' \end{pmatrix}\begin{pmatrix} \underline{d}' \\ \underline{d}'' \end{pmatrix} = \begin{pmatrix} U_y^{(f)} & -V_y^{(f)}Y_x \\ V_y^{(f)}Y_x & U_y^{(f)} \end{pmatrix}\begin{pmatrix} \underline{a}' \\ \underline{a}'' \end{pmatrix} + \begin{pmatrix} U_y^{(f)} & -V_y^{(f)}Y_x \\ -V_y^{(f)}Y_x & -U_y^{(f)} \end{pmatrix}\begin{pmatrix} \underline{b}' \\ \underline{b}'' \end{pmatrix} \tag{4.24b}$$

where 1 stands for the unit matrix. Eliminating $\underline{b}'$ and $\underline{b}''$ from the above two equations and invoking (4.23), we obtain:

$$\left[\begin{pmatrix} E'U_y' + \omega\mu U_y^{(f)}[K_t^{(f)}]^{-1}H' & S''V_y'' + \varepsilon_f V_y^{(f)} Y_x [K_t^{(f)}]^{-1} E''K_t'' \\ S'V_y' - \omega\mu V_y^{(f)}[K_t^{(f)}]^{-1}H' & H''U_y'' + \varepsilon_f U_y^{(f)}[K_t^{(f)}]^{-1}E''K_t'' \end{pmatrix}\right.$$

$$\left. + \begin{pmatrix} E'U_y' - U_y^{(f)}[K_t^{(f)}]^{-1}H' & S''V_y'' + \varepsilon_f V_y^{(f)} Y_x [K_t^{(f)}]^{-1} E''K_t'' \\ -S'V_y' + V_y^{(f)} Y_x [K_t^{(f)}]^{-1}H' & -H''U_y'' + \varepsilon_f U_y^{(f)}[K_t^{(f)}]^{-1}E''K_t'' \end{pmatrix}\begin{pmatrix} \Gamma_{11} & \Gamma_{12} \\ \Gamma_{21} & \Gamma_{22} \end{pmatrix}\right]\begin{pmatrix} \underline{c}' \\ \underline{c}'' \end{pmatrix}$$

$$= \begin{pmatrix} 2U_y^{(f)} & 0 \\ 0 & 2U_y^{(f)} \end{pmatrix}\begin{pmatrix} \underline{a}' \\ \underline{a}'' \end{pmatrix} \tag{4.25}$$

from which we can further obtain:

$$\begin{pmatrix} \underline{c}' \\ \underline{c}'' \end{pmatrix} = \begin{pmatrix} T_{11} & T_{12} \\ T_{21} & T_{22} \end{pmatrix}\begin{pmatrix} \underline{a}' \\ \underline{a}'' \end{pmatrix} \tag{4.26}$$

Finally, invoking (4.23) and (4.26), we obtain, from (4.24a)

$$\begin{pmatrix} \underline{b}' \\ \underline{b}'' \end{pmatrix} = \begin{pmatrix} R_{11} & R_{12} \\ R_{21} & R_{22} \end{pmatrix}\begin{pmatrix} \underline{a}' \\ \underline{a}'' \end{pmatrix} \tag{4.27a}$$

with

$$\begin{pmatrix} R_{11} & R_{12} \\ R_{21} & R_{22} \end{pmatrix} = \begin{pmatrix} 1 + \omega\mu H'(1+\Gamma_{11}) & -H'\Gamma_{12} \\ \varepsilon_f E''K_t''\Gamma_{21} & -1 + \varepsilon_f E''K_t''(1+\Gamma_{22}) \end{pmatrix}\begin{pmatrix} T_{11} & T_{12} \\ T_{21} & T_{22} \end{pmatrix} \tag{4.27b}$$

where the R's define the reflection coefficient matrices that properly take into account the coupling between the TE and TM modes. For a given plane wave incidence, $\underline{a}'$ and $\underline{a}''$ are known. The reflected harmonic amplitudes in the ε_f region is determined from (4.27a). The mode amplitudes in the grating region are determined from (4.26) and (4.23). The transmitted harmonic amplitudes are then determined from (4.21a) and (4.21c). The fields everywhere are thus completely determined.

B. Guidance of Waves Along a Periodic Dielectric Waveguide

A surface wave along a dielectric waveguide may be regarded as a plane wave being bounced back and forth within the waveguide, as depicted in Fig. 4.4 for a periodic dielectric waveguide. The scattering of the plane wave at the upper surface of the uniform layer, $z = 0$, has been analyzed in the preceding section and the scattering by the ground plane at $z = -t_f$ is a trivial problem that need not be discussed here. Making use of the known results of these scattering problems, we determine the dispersion relation for the periodic dielectric waveguide.

Referring to Fig. 4.4, at $z = 0$, the reflection coefficient matrix of the grating layer is defined in (4.27). Now, imagine that a set of incident plane waves characterized by the harmonic amplitude vectors $\underline{a}'$ and $\underline{a}''$ starts propagating in the forward direction at $z = 0$. While traversing the uniform layer, these plane waves will be reflected back and forth by the grating and the ground plane. Since the ground plane is taken as a perfect conductor, the reflection coefficient for every harmonic is equal to -1. For a guided wave, the harmonic amplitudes after a round-trip across the uniform layer must remain unchanged, e.g., we must have:

$$\begin{pmatrix} \underline{a}' \\ \\ \underline{a}'' \end{pmatrix} = - \begin{pmatrix} R_{11} & R_{12} \\ \\ R_{21} & R_{22} \end{pmatrix} \begin{pmatrix} e^{-j\,2K_z^{(f)} t_f} & 0 \\ \\ 0 & e^{-j\,2K_z^{(f)} t_f} \end{pmatrix} \begin{pmatrix} \underline{a}' \\ \\ \underline{a}'' \end{pmatrix} \tag{4.28}$$

where $K_z^{(f)}$ is a diagonal matrix with $k_{zn}^{(f)}$ as its element at the n-th diagonal position. Equation (4.28) is a homogeneous system of linear equations for which the existence of a nontrivial solution requires that the coefficient matrix be singular. After rearrangement, we obtain:

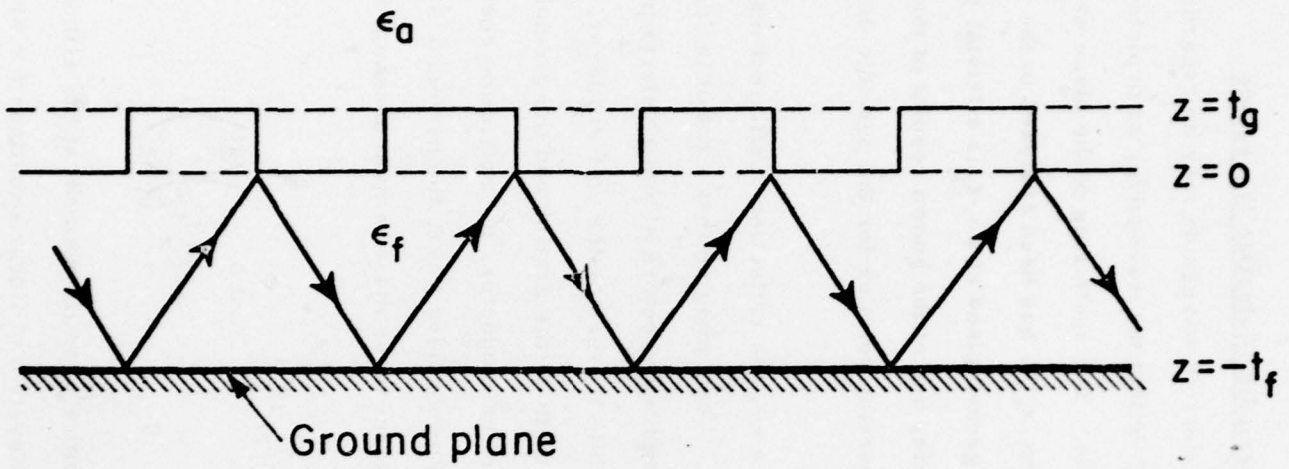

Fig. 4.4. Plane wave interpretation of a guided mode in a grating antenna.

$$\det\begin{pmatrix} 1 + R_{11}e^{-j2K_z^{(f)}t_f} & R_{12}e^{-j2K_z^{(f)}t_f} \\ R_{21}e^{-j2K_z^{(f)}t_f} & 1 + R_{22}e^{-j2K_z^{(f)}t_f} \end{pmatrix} = 0 \qquad (4.29)$$

which is the desired transverse resonance relation or the dispersion relation for the periodic dielectric waveguide. *It is noted that this is an exact dispersion* relation that applies to periodic dielectric waveguides of any structural parameters, including those of grating antennas for mm-wave applications. Also, for the special case of normal incidence, it can be shown that $R_{12} = R_{21} = 0$ and (4.29) is then reduced to the two dispersion relations:

$$\det(1 + R_{11}e^{-j2K_z^{(f)}t_f}) = 0 \qquad (4.30a)$$

$$\det(1 + R_{22}e^{-j2K_z^{(f)}t_f}) = 0 \qquad (4.30b)$$

for the decoupled TE and TM modes, respectively.

V. ACKNOWLEDGMENTS

This study was conducted during summer 1977 under the Laboratory Research Cooperative Program (LRCP).

References

1. S.T. Peng, T. Tamir and H.L. Bertoni, "Theory of Periodic Dielectric Waveguides," IEEE Trans. MTT, Vol. MTT-23, p. 123 (1975).

2. K. Honda, S.T. Peng and T. Tamir, "Improved Perturbation Analysis of Dielectric Gratings," Appl. Phys., Vol. 5, p. 325 (1975).

3. S.T. Peng and T. Tamir, "TM Mode Perturbation Analysis of Dielectric Gratings," Appl. Phys., Vol. 7, p. 35 (1975).

4. T. Tamir and S.T. Peng, "Analysis and Design of Grating Couplers," Appl. Phys., Accepted for publication.

IEEE TRANSACTIONS ON MICROWAVE THEORY AND TECHNIQUES, VOL. MTT-23, NO. 1, JANUARY 1975

APPENDIX

Theory of Periodic Dielectric Waveguides

S. T. PENG, MEMBER, IEEE, THEODOR TAMIR, SENIOR MEMBER, IEEE, AND HENRY L. BERTONI, MEMBER, IEEE

Abstract—**The propagation of electromagnetic waves along open periodic, dielectric waveguides is formulated here as a rigorous and exact boundary-value problem. The characteristic field solutions are shown to be of the surface-wave or leaky-wave type, depending on the ratio of periodicity to wavelength (d/λ). The dispersion curves and the space-harmonic amplitudes of these fields are examined for both TE and TM modes. Specific numerical examples are given for the cases of holographic layers and for rectangularly corrugated gratings; these show the detailed behavior of the principal field components and the dependence of waveguiding and leakage characteristics on the physical parameters of the periodic configuration.**

I. INTRODUCTION

THIN-FILM structures containing a periodic variation along the film have recently been of considerable interest in integrated optics because of the important role they play in applications such as beam-to-surface-wave couplers, filters, distributed feedback amplifiers and lasers, nonlinear generation of second harmonics, and beam reflection or steering devices of the Bragg type. The periodic variation is usually obtained by means of a dielectric grating, which is superimposed onto the upper surface of a layered configuration. This dielectric grating is in the form of a low-loss layer whose appearance falls into one of two categories: 1) the layer possesses parallel planar boundaries and its periodicity is produced by a longitudinal modulation of its refractive index (e.g., a bleached hologram), or 2) the layer contains a homogeneous medium but its upper boundary has a periodic variation (e.g., a grooved profile obtained by etching). Both types of construction of the dielectric layer are covered by the analysis presented here.

The operation of devices containing a dielectric grating depends on the properties of the electromagnetic fields guided by the structure. These fields appear either as surface waves, which travel parallel to the structure, or as leaky waves, which are guided by the structure but radiate or leak energy continuously into the exterior regions. Both types of waves appear as characteristic (free-resonant) solutions of the boundary-value problem prescribed by the thin-film configurations. Such problems have recently been considered [1]–[14] in the context of several specific structures, but most of the investigations have employed approximations that are too restrictive for many practical cases. The more common approximation has been the assumption that the grating periodicity acts as only a small perturbation in a configuration that, in the absence of the grating, appears as a planar multilayered medium [2], [3], [5], [9], [11], [12]. This approximation yields good results only if the periodic change is sufficiently small, so that its use may produce erroneous results in many practical cases, such as thick corrugated gratings having groove depths comparable to the wavelength [13], [14]. Another approximation has been the use of a Rayleigh assumption which incorrectly neglects the presence of incoming waves in the grating region [2], [4], [8]. It has been shown [10] that this Rayleigh approximation may also result in serious errors if the periodic variation is not sufficiently small. It should also be pointed out that most of the previous studies have developed their analysis in the context of *special* cases, which usually involved not more than three materials or layers; furthermore, some of these studies considered modes having one polarization only (usually the TE type) rather than both *TE and TM polarizations*.

The aim of this paper is to determine the wave-guiding properties of a very important class of dielectric gratings by utilizing a rigorous approach, which was briefly reported on recently in the specific context of modulated layers [6] and corrugated gratings [13], [14]. This approach does not employ any of the approximations mentioned above and it can be generalized to practically any planar dielectric grating. The generalization is accomplished by first considering both TE and TM modes in a canonic configuration consisting of a periodic layer bounded by two different media; the analysis is thereafter extended to structures with an arbitrary number of layered media, of which the grating configurations examined in the past represent special cases. A similar rigorous analysis has been reported by Neviere *et al.* [10], but their approach requires a numerical integration which may introduce certain inherent disadvantages. Although computer calculations may still be necessary to achieve highly accurate results with the method presented here, their precision can be easily and systematically obtained to any desired order. Furthermore, the solution is already in such a form that it lends itself readily to physical interpretations in terms of the effects due to the individual partial (space-harmonic) fields.

For surface waves and leaky waves supported by dielectric gratings, the two aspects of greatest interest are their dispersion curves and the amplitudes of their space harmonics. The dispersion curves dictate the proper conditions that must be satisfied for effective operation of any optical device employing periodic thin-film waveguides. The space-harmonic amplitudes determine whether the desired interaction is efficient or not. The derivation and calculation of both the dispersion curves and the

Manuscript received April 2, 1974; revised June 17, 1974. This work was supported in part by the U.S. Office of Naval Research, under Contract N00014-67-A-0438-0014, and in part by the U.S. Joint Services Electronics Program, under Contract F44620-69-C-0047.

The authors are with the Department of Electrical Engineering and Electrophysics, Polytechnic Institute of New York, Brooklyn, N.Y. 11201.

PRINTED IN THE U.S.A. Annals No. 501MT014

space-harmonic amplitudes are therefore presented here in detail, and several numerical examples are given to illustrate their variation with respect to the physical parameters of the periodic configurations. In particular, the role of the grating thickness is discussed and it is shown that the leakage of energy away from the structure is subject to a saturation effect which could not be evaluated by the approximate methods reported in the past.

II. CHARACTERISTIC FIELDS IN THE UNIFORM REGIONS AND THEIR PROPERTIES

The class of periodic thin-film structures considered here is depicted in Fig. 1, which shows structures consisting of one nonuniform (periodic) region and three uniform planar regions. The nonuniform region can be regarded as a planar layer of constant thickness t_g, whose composition varies periodically along x, with period d. The three uniform regions include a thin film of thickness t_f, an upper (air) half space, and a lower (substrate) region. In most practical cases, the substrate thickness is very much larger than the wavelength λ, so that the lower region may also be assumed to be a half space. However, the specific four-regions character of the structures shown in Fig. 1 is chosen here only because of its wide application and the results are generalized later to an arbitrary number of layers. If desired, the finite thickness of the substrate may then also be accounted for.

The fields supported by the structures in Fig. 1 are different in each of the four regions. To find a solution of the electromagnetic problem, it is therefore necessary to consider the type of (characteristic) waves that may appear in every separate region. The solution is then constructed by choosing a suitable combination of these waves so as to satisfy the boundary conditions. We shall therefore discuss here the type of fields that occur in the uniform regions, after which the fields in the periodic (grating) region will be examined in Section III. The boundary conditions and the derivation of the field solution is then given in Section IV, with discussions and numerical examples being presented in subsequent sections.

Because the widths (along y) of all the layers are large with respect to the wavelength λ, the fields are assumed to be invariant with respect to the y coordinate, i.e., $\partial/\partial y = 0$. For simplicity, we also assume that all of the media involved possess the permeability μ_0 of air (vacuum) and a time dependence $\exp(-i\omega t)$ is suppressed. If the periodic layer is absent, the field components of characteristic waves in the uniform layers appear in the form

$$F_j(x,z) = F_0^{(j)} \exp\left[i(k_x x + k_z^{(j)} z)\right] \tag{1}$$

where $F_0^{(j)}$ is a constant and

$$k_x^2 + [k_z^{(j)}]^2 = k_j^2 = k_0^2 \epsilon_j. \tag{2}$$

Here $k_0 = 2\pi/\lambda$ is the plane-wave propagation factor in air (vacuum) and the index j refers to the jth medium, with $j = a$ (air), f (film), or s (substrate). The quantity ϵ_j is the relative permittivity of the jth medium. In the absence of absorption and scattering losses, uniform layered structures can support surface waves that propagate without attenuation along x and decay away from the

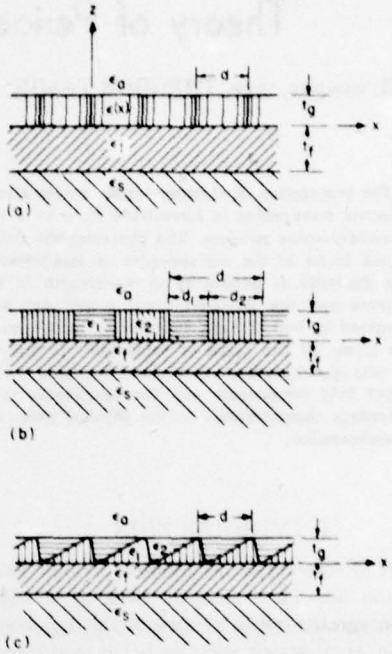

Fig. 1. Varieties of thin-film dielectric gratings. (a) Medium with periodic modulation of its permittivity. (b) Layer with rectangular corrugations. (c) Grating with curved profile.

structure in the air and substrate regions. These waves are therefore characterized by real values of $k_x = \beta_{xv}$ and imaginary values of $k_z^{(j)}$ for $j = a$ and $j = s$.

When a grating is superimposed on the uniform layered structure, the surface-wave field is modified to satisfy the periodic boundary conditions on the grating. Under those conditions, the field in all of the uniform regions (i.e., everywhere except within the grating layer) must appear in the Floquet form

$$F_j(x,z) = \sum_n F_n^{(j)} \exp\left[i(k_{xn} x + k_{zn}^{(j)} z)\right], \qquad (j \neq g) \tag{3}$$

where the amplitudes $F_n^{(j)}$ of each partial field in the above summation can be found by satisfying both the boundary conditions at each interface and the periodic conditions imposed by the grating. The index n under the summation sign is understood to run over all values of $n = 0, \pm 1, \pm 2, \cdots$, this convention being followed throughout this work unless otherwise stated. The quantities k_{xn} are related to the fundamental longitudinal factor k_{x0} by the Floquet condition

$$k_{xn} = k_{x0} + 2n\pi/d, \qquad (n = 0, \pm 1, \pm 2, \cdots). \tag{4}$$

Because $F_j(x,z)$ must satisfy the Helmholtz equation

$$\nabla^2 F_j + k_j^2 F_j = 0 \tag{5}$$

each partial wave now obeys the dispersion relation (2), which yields

$$k_{zn}^{(j)} = \pm (k_j^2 - k_{xn}^2)^{1/2} \tag{6}$$

where the sign in (6) is chosen so that, for real values of k_{x0}, $k_{zn}^{(j)}$ is either positive real or positive imaginary. For complex values of k_{x0}, however, the choice of sign is given by (10), as discussed later.

We observe that each nth partial field in (3) may be regarded as a mode with transverse variation $\exp(ik_{xn}x)$ along x, which propagates along z with a propagation factor $k_{zn}^{(j)}$. Hence, within a finite-thickness layer (such as that of thickness t_f in Fig. 1), *both signs in (6) must be* accounted for because they refer to waves that travel along the $+z$ or the $-z$ directions. In such a case, each nth term in (3) includes two separate components, one each for the $+z$ and $-z$ directions. In the open (air and substrate) regions, on the other hand, it is necessary to retain only that component whose energy flow or decay is away from the structure.

If the grating layer is sufficiently thin, the fundamental propagation factor k_{x0} is very closely given by the propagation factor β_{sw} of the surface wave on the uniform layered structure (with no grating). Also, the fields of the fundamental ($n = 0$) partial wave are evanescent with respect to z in the air and substrate regions. However, even a very thin grating requires the presence of all k_{xn} to satisfy the appropriate boundary conditions; for such a thin grating, all higher ($n \neq 0$) coefficients $F_n^{(j)}$ generally *possess very small magnitudes. Nevertheless,* some of these higher order partial waves may modify the nature of the guided waves. This is seen from (6) where, if we assume that $k_{x0} = \beta_{sw}$, we find that $k_{zn}^{(j)}$ may be real for $j = a,s$ if n is negative and the periodicity length d is sufficiently small. In the air and substrate regions, a real value for $k_{zn}^{(j)}$ implies that the nth field component propagates along z, in contrast to the fundamental ("surface-wave") component $n = 0$ which is evanescent along z. The propagating nth component accounts for energy that flows away from the structure, so that the complete field given by (3) is then no longer a true surface wave because now not all of the energy flows parallel to the x direction.

The foregoing features may be clarified by considering a surface wave incident from the left on a uniform structure, as shown in Fig. 2. For $x > 0$, a grating is superposed on the structure but we may first assume that this grating

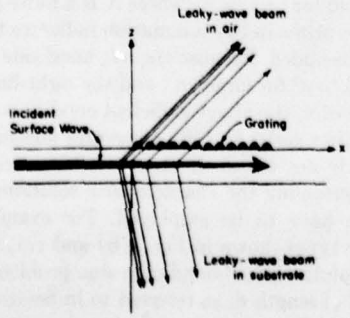

Fig. 2. Surface wave incident from a uniform region ($x < 0$) onto a region containing a periodic perturbation ($x > 0$). The periodicity modifies the surface-wave field by leaking beams at angles $\theta_n^{(j)}$ in the air and substrate regions ($j = a, s$). For clarity, only one such beam is shown in each region. The arrows suggest energy flux.

consists of very small periodic perturbations of the layer that supports the surface wave. Hence, as the surface wave enters into and progresses along the grating portion, a very small amount of field scattering occurs at every perturbation. Because this scattering is very weak, the surface-wave field in the grating region is, on a local scale, essentially quite similar to that in the nonperiodic ($x < 0$) portion. However, if the grating region is long, the energy *leaked by scattering adds up to a large portion of the* energy brought into the grating region by the incident surface wave. Because of the regular placement of the scatterers, the individually scattered fields interfere constructively only along certain preferred directions and the leaked energy appears in the form of beams that radiate at angles $\theta_n^{(j)}$, which are given by

$$\tan \theta_n^{(j)} = k_{xn}/k_{zn}^{(j)}. \tag{7}$$

Here $\theta_n^{(j)}$ is a real angle only for real values of $k_{zn}^{(j)}$. Along these real angles $\theta_n^{(j)}$, an energy flux appears in the form of radiation in the air ($j = a$) or in the substrate ($j = s$) regions.

The foregoing argument implies that, because energy loss occurs due to radiation, the complete guided field must decay with x as it progresses along the grating region. Hence, the propagation factor k_{x0} along the grating region cannot remain purely real but, instead, k_{x0} is changed from the value β_{sw} of the surface wave to a complex value. We therefore obtain

$$k_{xn} = \beta_n + i\alpha = (\beta_0 + 2n\pi/d) + i\alpha \tag{8}$$

where the imaginary term $\alpha > 0$ is responsible for the decay due to radiation leakage. We note that (8) indicates that the longitudinal decay factor α is the same for all of the partial field components in (3), as required by the *Floquet condition (4). Evidently, (6) implies that* $k_{zn}^{(j)}$ is then also complex, so that

$$k_{zn}^{(j)} = \xi_n^{(j)} + i\eta_n^{(j)}. \tag{9}$$

We now note that, unlike α, the transverse decay factor $\xi_n^{(j)}$ is generally different for every n. It is also important to recognize that α is small in the case of thin gratings (i.e., small periodic scatterers), but η_n may be large or small depending on n. Because $k_{zn}^{(j)}$ is complex, the square-root sign in (6) must be selected to satisfy[1]

$$\eta_n \gtrless 0 \quad \text{as} \quad \beta_n \gtrless 0. \tag{10}$$

Because waves guided by periodic structures generally contain radiating field components, these waves are no longer true surface waves (with k_{x0} = real). Instead, they are referred to as leaky waves (with k_{x0} complex). Although these leaky waves were described above in terms of *small periodic perturbations, it should be evident that* the foregoing argument also holds for large periodic scatterers because the size of the perturbations affects the leaky waves only quantitatively. Thus the leakage parameter α and the higher order ($n \neq 0$) amplitudes $F_n^{(j)}$ are small only in the case of small perturbations; as the size

[1] This choice requires an analytical continuation argument for k_{zn}, as discussed in [25].

of the scatterers increases, α and $F_n^{(3)}$ generally also increase and the overall leakage effect becomes more pronounced.

III. CHARACTERISTIC FIELDS IN THE GRATING REGION

To find the fields supported by the entire thin-film structure, it is necessary to examine the characteristic waves in the periodic layer, which will be henceforth referred to as the grating region. As two-dimensional (y-invariant) fields can be decomposed into TE and TM modes, the Maxwell equations for the field vectors can be reduced to the scalar equation

$$\nabla^2 F_y + k^2(x) F_y = 0 \tag{11}$$

where now $k^2(x)$ is no longer a constant as in (5). We shall restrict the present discussion to gratings of the type shown in Fig. 1(a) and (b), for which $k^2(x)$ is a function of x only. The procedure for extending our results to the more general case having also a z dependence, as is the case in Fig. 1(c), is discussed later in Section IIIC. The electric and magnetic fields $\boldsymbol{E}$ and $\boldsymbol{H}$, and the parameter $k(x)$ are then specified as follows.

TE modes:

$$\boldsymbol{E} = \boldsymbol{y}_0 F \quad \text{and} \quad \boldsymbol{H} = -\frac{i}{\omega\mu_0} \nabla \times \boldsymbol{E} \tag{12}$$

$$k^2(x) = k_0^2 \epsilon(x). \tag{13}$$

TM modes:

$$\boldsymbol{H} = \boldsymbol{y}_0 \epsilon^{1/2}(x) F \quad \text{and} \quad \boldsymbol{E} = \frac{i}{\omega\epsilon(x)} \nabla \times \boldsymbol{H} \tag{14}$$

$$k^2(x) = k_0^2 \epsilon(x) - \frac{3}{4}\left[\frac{\epsilon'(x)}{\epsilon(x)}\right]^2 + \frac{\epsilon''(x)}{2\epsilon(x)}. \tag{15}$$

Here $\boldsymbol{y}_0$ is a unit vector along y and $\epsilon(x)$ denotes the relative permittivity in the grating region, whose x-dependent behavior is discussed further below in the context of specific examples.

As indicated by (11)–(15), a key step in finding the characteristic solution $F_y = F_y(x,z)$ in the grating region requires the specification of $k(x)$ via $\epsilon(x)$. Because $\epsilon(x)$ is periodic, $k(x)$ can be generally represented by a Fourier series such that

$$k^2(x) = k_0^2 \sum_n p_n \exp(i2n\pi x/d) \tag{16}$$

where the coefficients p_n are known for a given grating. We may then take

$$F_y = \sum_n q_n(z) \exp(ik_{xn}x) \tag{17}$$

where k_{xn} was defined in (4). Inserting this representation into (11), we obtain the system of differential equations

$$\frac{d^2}{dz^2}\boldsymbol{q} = -\boldsymbol{P}\boldsymbol{q} \tag{18}$$

where $\boldsymbol{q} = \boldsymbol{q}(z)$ is a column vector with elements $q_n(z)$ and $\boldsymbol{P} = (P_{nl})$ is a constant matrix (independent of z) whose elements are defined by

$$P_{nl} = k_0^2 p_{n-l} - k_{xn}^2 \delta_{nl}. \tag{19}$$

The system of differential equations (18) characterizes the couplings between all of the space harmonics in the grating region. As a result of this coupling, the variation with respect to z of the waves is considerably more complicated in the grating region than in any of the uniform layers. To solve the coupled system of differential equations with constant coefficients, we may assume a solution of the form

$$\boldsymbol{q} = \boldsymbol{c} \exp(i\kappa z) \tag{20}$$

where κ is a propagation constant along z in the grating region, and $\boldsymbol{c}$ is a constant vector (independent of z). Substituting (20) into (18), we obtain system of linear homogeneous equations

$$\boldsymbol{P}\boldsymbol{c} = \kappa^2 \boldsymbol{c} \tag{21}$$

which states that κ^2 is an eigenvalue of the matrix $\boldsymbol{P}$. We therefore obtain the characteristic equation

$$\det[\boldsymbol{P} - \kappa^2 \boldsymbol{1}] = 0 \tag{22}$$

where 1 is a unit matrix of infinite order. Let κ_m^2 be an eigenvalue determined from (22); the corresponding eigenvector $\boldsymbol{c}_m$ (with elements c_{mn}) can then be obtained by solving the system of linear homogeneous equations (21). From (20), we thus have a pair of eigensolutions

$$\boldsymbol{q}_m^{(+)}(z) = \boldsymbol{c}_m \exp(i\kappa_m z) \tag{23a}$$

$$\boldsymbol{q}_m^{(-)}(z) = \boldsymbol{c}_m \exp(-i\kappa_m z). \tag{23b}$$

The sign of κ_n is chosen according to (9) and (10). Thus the + and − signs in $q_m^{(\pm)}(z)$ represent waves that travel along the positive and negative directions of the z axis, respectively.

An inspection of the matrix $\boldsymbol{P}$ reveals that the determinant in (22) is of the Hill type, so that the eigenvalues κ_m^2 may be evaluated by a judicious truncation of the determinant. By extending to the present case a theorem on infinite determinants [15], we find that such a truncation is valid provided

$$(1/k_0^2)\,|\,k_0^2 p_0 - k_{xn}^2 - \kappa^2\,| > \sum_i{}' |\,p_i\,| \tag{24}$$

which must hold for $|\,n\,| > N$, where N is a finite positive integer and the prime in the summation indicates that the term $i = n$ is excluded. Because the left-hand side in (24) is proportional to n^2 for large $|\,n\,|$ and the right-hand side is independent of n, the above sufficient condition is satisfied if the Fourier series in (16) converges absolutely. If this condition is not satisfied, other mathematical techniques for determining the characteristic solutions in the grating region have to be employed. For example, for gratings of the types shown in Fig. 1(b) and (c), we may resort to the solution of a boundary-value problem for an individual cell of length d, as referred to in Section IIIB.

We recall that the vector $\boldsymbol{c}_m$ contains elements c_{mn}, so that every complete (modal) mth solution F_y in the grating region contains an infinite set of space harmonics, each of which has an amplitude c_{mn}. This is in contrast to

the fields F_j in the other (uniform) regions ($j \neq g$) wherein every nth mode contains a single space harmonic, which forms by itself an independent solution of the pertinent wave equation. After determining the values of κ_m from (22), all of the coefficients c_{mm} can also be found by using (21) which specifies these coefficients as ratios with respect to one of them, say c_{mn}. The value of c_{mm} can itself be prescribed by a normalization condition, which may be chosen to be $c_{mm} = 1$ for the present class of problems. However, it is important to recognize that all κ_m and c_{mn} can be found and may be assumed known if $\epsilon(x)$ is specified in (11)–(15).

To illustrate the foregoing concepts, we shall consider the specific grating structures shown in Fig. 1, which are of current practical interest.

A. *Sinusoidally Modulated Medium*

For the periodic layer of holographic type, which appears in the structure of Fig. 1(a), a canonic description of its medium is given by

$$\epsilon(x) = \epsilon_g \left(1 + M \cos \frac{2\pi}{d} x\right) \tag{25}$$

where ϵ_g is the average relative permittivity and M is the modulation index.

The propagation of TE waves in such a medium has been extensively investigated by Tamir *et al.* [16]; in this case, the Hill's determinant yielding κ_m and the Fourier coefficients c_{mn} can be conveniently analyzed in terms of rapidly convergent continued fractions. The results have then been applied by Wang [17] to the solutions of TE waves guided by a slab of the modulated medium in a uniform and symmetric environment.

For TM waves, on the other hand, the Hill's determinant has been analyzed by Yeh *et al.* [18], but the harmonic amplitudes c_{mn} have not been studied. Recently, a new formulation for this TM-wave problem has been presented by Peng and Hessel [19]. This new method of analysis is particularly useful for analytically determining the space-harmonic amplitudes c_{mn} of the electromagnetic fields. Thus the boundary value problem for this class of dielectric waveguides can now be rigorously treated for TM waves, in a manner analogous to that of TE waves.

B. *Rectangularly Modulated Medium*

The variation of the medium that forms the grating in Fig. 1(b) can be described by a rectangular modulation, which is given by

$$\epsilon(x) = \epsilon_1 + (\epsilon_2 - \epsilon_1) \sum_l [U(x - ld) - U(x - ld - d_1)] \tag{26}$$

where $U(x)$ is the unit step function of argument x. In current practice, $\epsilon_1 = \epsilon_a$ and $\epsilon_2 = \epsilon_f$, but we shall here let both ϵ_1 and ϵ_2 be arbitrary so as to cover a larger class of applications.

If the thickness t_g of the grating region is made infinitely large, we obtain a periodic array of dielectric slabs, whose characteristic waves have been examined by Lewis and Hessel for TM modes [20]. In this case, both the dispersion relation for obtaining κ_m and the harmonic amplitudes c_{mn} can be found in terms of closed-form solutions. Hence the solution of the set of equations (21) and their associated Hill's determinant (22) can be dispensed with and the closed forms derived by Lewis and Hessel may be used instead.

Although TE modes have not been explicitly examined by Lewis and Hessel, their analysis is analogous to that of TM modes. Thus, for structures with rectangular corrugations of the type shown in Fig. 1(b), the characteristic waves that appear in the grating region are known, as was also the case for structures with a sinusoidally modulated layer.

C. *Curved-Profile Gratings*

Because the foregoing two grating profiles possess functions $\epsilon(x)$ that are invariant with z, they lend themselves directly to a rigorous solution of the boundary-value problem. In contrast, the curved profile of Fig. 1(c) is generally not separable with respect to the x and z coordinates and has been solved, so far, only by employing numerical integrations [10]. Nevertheless, the approach described here can be generalized to also solve curved profiles by using judicious approximations of these profiles.

To illustrate this generalization, consider the grating with slanted boundaries in Fig. 3(a). By partitioning the grating into fine layers and approximating each of these by rectangular profiles, we obtain a configuration as indicated in Fig. 3(b). Although now we have more than a single periodic layer, each one of them has a rectangular shape like that in Fig. 1(b) and, furthermore, all of the layers have the same periodicity d. The analysis of the multiply layered grating then follows as a straightforward extension of that for the single grating, as discussed in Section VB. Although this extension is only an approximation for the original slanted grating, this approximation can be made as accurate as desired by subdividing the grating into sufficiently many fine layers.

A much simpler, but probably less accurate, procedure for treating a curved-profile grating is to average (for

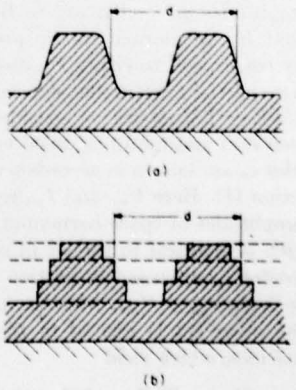

Fig. 3. Approximation of a curved profile by periodic layers with rectangular shapes. (a) Actual profile. (b) Approximated profile.

every x) the permittivity over z inside the grating layer. Thus, if the profile of the periodic boundary that separates the two media with permittivities ϵ_1 and ϵ_2 in Figs. 1(c) or 3(a) is described by the function

$$z = h(x) = h(x + d), \qquad \text{for } 0 \leq z \leq t_g \tag{27}$$

the averaged permittivity becomes

$$\epsilon(x) = \epsilon_2 + (\epsilon_2 - \epsilon_1)\frac{h(x)}{t_g}. \tag{28}$$

The problem is then reduced to that of a layer with uniform thickness but with varying $\epsilon(x)$, as was the case of the modulated medium in Section IIIC above, except that $\epsilon(x)$ in (28) may contain many sinusoidal terms. Nevertheless, this problem lends itself to the same treatment involving Hill's functions as the TM modes discussed by Yeh *et al.* [18] and Peng *et al.* [19].

IV. FIELD SOLUTION FOR PERIODIC LAYERS

After specifying the fields within the separate layers of a dielectric grating structure, we may now consider the boundary-value problem. For this purpose, we simplify the problem by considering first a single periodic layer adjacent to two half spaces, as shown in Fig. 4. In this case, a single periodic layer of thickness t_g is left. The presence of one (or more) uniform layers is then accounted for in Section V by straightforward modifications of the formal rigorous solution of the electromagnetic problem posed by Fig. 4.

Within the periodic (grating) layer, (17) and (23) imply that the electric and magnetic field components transverse to z are, respectively, given by

$$E_g = \sum_m \left[g_m^{(+)} \exp\,(i\kappa_m z) + g_m^{(-)} \exp\,(-i\kappa_m z)\right] \sum_n V_{mn} \exp\,(ik_{xn}x) \tag{29}$$

$$H_g = \sum_m \left[g_m^{(+)} \exp\,(i\kappa_m z) - g_m^{(-)} \exp\,(-i\kappa_m z)\right] \sum_n I_{mn} \exp\,(ik_{xn}x). \tag{30}$$

The above is a modal representation that regards the fields in terms of modes that propagate in the z direction, each mth term in the first summation being an independent mode with amplitudes $g_m^{(\pm)}$ that are to be determined. Because E_g and H_g are normal to the propagation (z) direction, they correspond to either F_g, discussed in Section III, or to its partial z derivative, depending on which of the specific TE or TM modes are considered.

For any given $\epsilon(x)$ and for an assumed value of k_{x0}, all of the quantities κ_m are known in accordance with the discussion in Section III. Here V_{mn} and I_{mn} refer to voltage and current amplitudes of space harmonics, respectively, one set of which is identical to the set of coefficients c_{mn} forming the vector c_m discussed in Section III; thus, for TE modes we have $c_{mn} = V_{mn}$, whereas for TM modes $c_{mn} = I_{mn}$. The other set is related to the first set via Maxwell's equations, which yield

$$V_{mn} = \sum Z_{m,n-r}^{(g)} I_{nr} \tag{31}$$

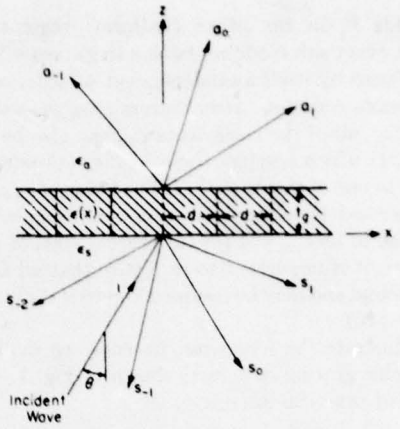

Fig. 4. Canonic configuration containing a single periodic layer of thickness t_g.

where $Z_{m,n-r}^{(g)}$ is an impedance that represents the coupling of the rth harmonic of the magnetic field to the nth harmonic of the electric field. The value of $Z_{m,n-r}^{(g)}$ is determined by the specific relationship that relates E_g and H_g for each mode via Maxwell's equations (12) and (14). For example, in the case of a sinusoidally modulated layer of the type discussed in Section IIIA, we get

$$Z_{m,n-r}^{(g)} = \begin{cases} [\omega\mu_0/k_{zm}^{(g)}]\delta_{nr}, & \text{for TE modes} \\ [k_{zm}^{(g)}/\omega\epsilon_0\epsilon_g][\delta_{nr} + M(\delta_{n-1,r} + \delta_{n+1,r})], & \text{for TM modes} \end{cases} \tag{32}$$

where δ_{nr} is Kronnecker's delta function. For convenience, we assume now that we wish to solve the fields due to a plane wave incident at an angle θ from the substrate region, as shown in Fig. 4. In this case, $k_{x0} = k_s \sin\theta$ refers to the wavenumber along x dictated by the incident wave and, in view of (3) in Section II, the fields in the substrate are given by

$$E_s = \exp\,(ik_{x0}x + ik_{z0}^{(s)}z) + \sum_n s_n \exp\,(ik_{xn}x - ik_{zn}^{(s)}z) \tag{33}$$

$$H_s = Y_0^{(s)} \exp\,(ik_{x0}x + ik_{z0}^{(s)}z) - \sum_n s_n Y_n^{(s)} \exp\,(ik_{xn}x - ik_{zn}^{(s)}z) \tag{34}$$

where it is assumed that the incident wave amplitude is unity and the amplitudes s_n of the scattered waves have to be determined. The fields in the air region are given by

$$E_a = \sum_n a_n \exp\,(ik_{xn}x + ik_{zn}^{(a)}z) \tag{35}$$

$$H_a = \sum_n a_n Y_n^{(a)} \exp\,(ik_{xn}x + ik_{zn}^{(a)}z) \tag{36}$$

where k_{xn} and $k_{zn}^{(j)}$ were defined in (4) and (6), $Y_n^{(j)}$ is now the characteristic modal admittance

$$Y_n^{(j)} = \begin{cases} k_{zn}^{(j)}/\omega\mu_0, & \text{for TE modes} \\ \omega\epsilon_0\epsilon_j/k_{zn}^{(j)}, & \text{for TM modes} \end{cases} \qquad (j \neq g) \tag{37}$$

and the amplitudes a_n are to be determined together with

s_n and $g_m^{(\pm)}$ by matching the boundary conditions, which require that the appropriate components in (29), (30), and (33)–(36) be continuous at $z = 0$ and t_g. This leads to the following systems of equations:

$$\delta_{0n} + s_n = \sum_m V_{mn}[g_m^{(+)} + g_m^{(-)}] \tag{38}$$

$$Y_n^{(a)}(\delta_{0n} - s_n) = \sum_m I_{mn}[g_m^{(+)} - g_m^{(-)}] \tag{39}$$

$$\sum_m V_{mn}[\exp(i\kappa_m t_g) g_m^{(+)} + \exp(-i\kappa_m t_g) g_m^{(-)}] = \exp(ik_{zn}^{(a)} t_g) a_n \tag{40}$$

$$\sum_m I_{mn}[\exp(i\kappa_m t_g) g_m^{(+)} - \exp(-i\kappa_m t_g) g_m^{(-)}] = \exp(ik_{zn}^{(a)} t_g) Y_n^{(a)} a_n \tag{41}$$

for all $n = 0, \pm 1, \pm 2, \cdots$. These are the four coupled systems of linear equations that determine the four sets of unknown scattered harmonic amplitudes a_n, s_n, $g_n^{(+)}$, and $g_n^{(-)}$, as follows.

Multiplying (40) by $Y_n^{(a)}$ and then subtracting the resulting equation from (41), we obtain, in matrix notation,

$$\boldsymbol{g}^{(-)} = \exp(i\boldsymbol{K}_g t_g) \boldsymbol{R}_g \exp(i\boldsymbol{K}_g t_g) \boldsymbol{g}^{(+)} \tag{42}$$

where $\boldsymbol{g}^{(\pm)}$ are column matrices with elements $g_m^{(\pm)}$, $\exp(i\boldsymbol{K}_g t_g)$ is a diagonal matrix with elements $\delta_{mn} \exp(i\kappa_m t_g)$ and $\boldsymbol{R}_g$ is the reflection coefficient matrix looking into the air region at $z = t_g$, as given by

$$\boldsymbol{R}_g = (\boldsymbol{I} + \boldsymbol{Y}_a \boldsymbol{V})^{-1}(\boldsymbol{I} - \boldsymbol{Y}_a \boldsymbol{V}) \tag{43}$$

with $\boldsymbol{I}$ and $\boldsymbol{V}$ being square matrices with elements $(\boldsymbol{I})_{mn} = I_{nm}$ and $(\boldsymbol{V})_{mn} = V_{nm}$, respectively, and $\boldsymbol{Y}_a$ being a diagonal matrix with elements $Y_n^{(a)} \delta_{mn}$.

Next, we multiply (38) by $Y_n^{(a)}$, add the result to (39) and invoke (42) to obtain

$$\boldsymbol{S}_g \boldsymbol{g}^{(+)} = \boldsymbol{T}_0 \boldsymbol{e} \tag{44}$$

with

$$\boldsymbol{S}_g = \boldsymbol{1} - \boldsymbol{R}_0 \exp(i\boldsymbol{K}_g t_g) \boldsymbol{R}_g \exp(i\boldsymbol{K}_g t_g) \tag{45}$$

$$\boldsymbol{T}_0 = 2(\boldsymbol{I} + \boldsymbol{Y}_s \boldsymbol{V})^{-1} \boldsymbol{Y}_s \tag{46a}$$

$$\boldsymbol{R}_0 = (\boldsymbol{I} + \boldsymbol{Y}_s \boldsymbol{V})^{-1}(\boldsymbol{I} - \boldsymbol{Y}_s \boldsymbol{V}). \tag{46b}$$

Here $\boldsymbol{e}$ is a column vector with elements δ_{0n}, $\boldsymbol{Y}_s$ is a diagonal matrix with elements $Y_n^{(s)} \delta_{mn}$, while $\boldsymbol{T}_0$ and $\boldsymbol{R}_0$ are, respectively, transmission and reflection matrices looking down into the substrate at $z = 0$.

When the matrix $\boldsymbol{S}_g$ in (44) is singular, the fields are in resonance as discussed in Section V. For nonresonant fields, the inverse of $\boldsymbol{S}_g$ exists and $\boldsymbol{g}^{(+)}$ is then uniquely determined via (44) for plane-wave incidence. Using (42) and (44), we then obtain from (38) that the scattered field amplitudes s_n in the substrate are given by the column vector

$$\boldsymbol{s} = \bar{\boldsymbol{R}}_0 \boldsymbol{e} \tag{47a}$$

where $\bar{\boldsymbol{R}}_0$ is a reflection matrix looking up at $z = 0$, as given by

$$\bar{\boldsymbol{R}}_0 = \boldsymbol{T}_0^{-1}[\exp(i\boldsymbol{K}_g t_g) \boldsymbol{R}_g \exp(i\boldsymbol{K}_g t_g) - \boldsymbol{R}_0] \boldsymbol{S}_g^{-1} \boldsymbol{T}_0. \tag{47b}$$

If required, the scattered amplitudes a_n in the air can be similarly obtained via (40) or (41), together with (42) and (44). This would complete the determination of all the scattered amplitudes a_n, $g_m^{(\pm)}$, and s_n.

V. THE FIELDS GUIDED BY DIELECTRIC GRATINGS

As discussed in the Introduction, the fields of greatest interest are those that can be supported by periodic thin-film structures in the absence of any wave incident from the air or the substrate. These fields are those of the surface and leaky waves described in Section II, which represent free-resonant solutions of the boundary-value problem under consideration. We shall discuss these solutions first for the canonic structure shown in Fig. 4, after which we shall generalize the result to structures with an arbitrary number of layers in addition to the single periodic layer of Fig. 4.

A. Guiding by a Single Periodic Layer

In the absence of a wave incident from an exterior region, we have a null vector instead of $\boldsymbol{e}$ in (44), which is then satisfied only if the determinant of $\boldsymbol{S}_g$ vanishes, namely,

$$\det(\boldsymbol{S}_g) = \det[\boldsymbol{1} - \boldsymbol{R}_0 \exp(i\boldsymbol{K}_g t_g) \boldsymbol{R}_c \exp(i\boldsymbol{K}_g t_g)] = 0. \tag{48}$$

This represents the dispersion relation for the guided (surface or leaky) waves of the grating in Fig. 4. This relation yields the unknown eigenvalues k_{z0}. For any such k_{z0}, we can then find all $g_n^{(+)}$ in terms of one of them by replacing $\boldsymbol{e}$ by $\boldsymbol{0}$ in (44). All of the other amplitudes a_n, $g_n^{(-)}$, and s_n can thereafter be determined as discussed at the end of the preceding section.

Because the foregoing analysis regards the fields as propagating along the z direction, which is normal to the boundaries, the result of (48) represents the transverse resonance condition for the present configuration. To understand the physical significance of this condition, let us consider the special case when the periodic layer in Fig. 4 is replaced by a uniform slab (with no periodic variation). In this case, (48) reduces to

$$1 - r_0 r_g \exp(2i\kappa t_g) = 0 \tag{49}$$

where r_0 and r_g are reflection coefficients looking into the substrate and air regions, respectively, at $z = 0$ and t_g. Equation (49) states the familiar (resonant, surface-wave) condition that the wave remains unchanged after a round-trip travel across the layer, the trip including one reflection at each of the two boundaries [21]. Thus (48) for the grating layer is a generalization of (49) for the uniform layer. The transition from scalars in (49) to matrices in (48) represents the fact that the presence of periodicity introduces energy coupling from the fundamental ($n = 0$) field to its higher order ($n \neq 0$) space harmonics.

In the case of a uniform layer, (49) is a transcendental equation, which may be solved graphically or numerically to find the propagation factor along the structure. For a periodic layer, (48) is considerably more complicated

because it involves an infinite determinant which must be truncated to solve for the unknown propagation factor k_{z0}. This determinant is also of the Hill's type, as was the case in (22), so that its truncation can be carried out very accurately by numerical computer techniques, as discussed further in Section VI.

B. Guiding by Multilayered Periodic Structures

The results discussed in the preceding section may now be extended to structures that possess several layers which are additional to the single nonuniform (periodic) layer discussed above. For this purpose, we first recognize that the electromagnetic problem of the single periodic layer may be rigorously described by the equivalent transverse network shown in Fig. 5(a). In this network, each of the semi-infinite transmission line in the air or substrate regions represents one of the modes; the characteristic admittance $Y_n^{(s)}$ and propagation factor $k_{zn}^{(s)}$ have been defined in (37) and (6), respectively. All of these transmission lines are connected to the grating region, which is now represented schematically by the box marked B in Fig. 5(a).

If desired, the network describing the scattering properties of the box marked B can be synthesized along the lines discussed in [22] for the case of an interface to a sinusoidally modulated medium. However, this synthesis is not necessary for the purposes of the present work because we may regard the box marked B in Fig. 5(a) to be defined by (47) for $\boldsymbol{S}_g$. We note, on the other hand, that the matrix $\boldsymbol{S}_g$ describes the coupling of all of the modes to each other via the periodic properties of the grating region.

To generalize the result to additional uniform layers, consider now the structures described in Fig. 1(a) and 1(b). These configurations can be represented by the equivalent network of Fig. 5(b), which is obtained by simply interposing an appropriate set of transmission lines of lengths t_f between the grating and substrate regions. In this case, we may look down at the plane $z = -t_f$ and define a reflection coefficient

$$\rho_n = \frac{Y_n^{(f)} - Y_n^{(s)}}{Y_n^{(f)} + Y_n^{(s)}}. \tag{50}$$

By utilizing ρ_n, we obtain that the input admittance $Y_n^{(in)}$ at $z = 0$ in every transmission line is given by

$$Y_n^{(in)} = \frac{1 - \rho_n \exp(2ik_{zn}^{(f)}t_f)}{1 + \rho_n \exp(2ik_{zn}^{(f)}t_f)} Y_n^{(f)}. \tag{51}$$

We can use now (45) for $\boldsymbol{R}_0$ and replace $Y_n^{(s)}$ therein with $Y_n^{(in)}$ to get the modified reflection matrix $\boldsymbol{R}_0'$ for the (two-layer) configurations of Fig. 1 in the form

$$\boldsymbol{R}_0' = (\boldsymbol{I} + \boldsymbol{Y}_{in}\boldsymbol{V})^{-1}(\boldsymbol{I} - \boldsymbol{Y}_{in}\boldsymbol{V}) \tag{52}$$

where $\boldsymbol{Y}_{in}$ is a diagonal admittance matrix with elements $Y_n^{(in)}\delta_{mn}$. By next taking $\boldsymbol{R}_0'$ instead of $\boldsymbol{R}_0$ in (48), the transverse resonance condition is extended to the geometries of Fig. 1, which possess the additional uniform layer of thickness t_f.

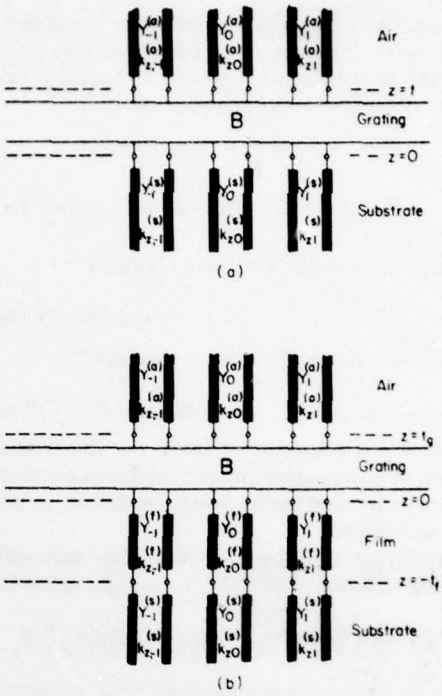

Fig. 5. Equivalent transverse networks for the analysis of dielectric-grating structures. (a) Network for the single-layer configurations of Fig. 3. (b) Network for the structures shown in Fig. 1.

The above procedure can, of course, be generalized to any number of layers that are added below the film layer. As suggested by Fig. 5, all that is needed is to modify $\boldsymbol{R}_0'$ so as to take into account the additional layers. As such a modified expression for $\boldsymbol{R}_0'$ involves the input admittances $Y_n^{(in)}$ looking into a stack consisting of an arbitrary number of uniform layers, the extension is straightforward. The same procedure can be utilized if additional uniform layers are placed above (rather than below) the grating region. In this case, the reflection matrix $\boldsymbol{R}_g$ must be modified to a matrix $\boldsymbol{R}_g'$ in a manner analogous to that discussed above for $\boldsymbol{R}_0'$. Of course, uniform layers may be accommodated both below and on top of the grating layer by employing the appropriate modified expressions $\boldsymbol{R}_0'$ and $\boldsymbol{R}_g'$ at the respective boundaries of the grating region.

Finally, additional periodic (rather than uniform) layers can also be accommodated in order to treat structures discussed in Section IIIC. This extension is somewhat more complicated because now we connect additional boxes of the form marked B in Fig. 5 rather than just transmission line sections. In matrix notation, this extension is nevertheless conceptually straightforward and the resulting expressions are relatively simple if all the periodic layers possess the same periodicity d, as prescribed in Section IIIC. As such an extension is beyond the scope of this paper, the interested reader should consult reference [23] for further details.

VI. DERIVATION OF NUMERICAL RESULTS

The application of the techniques described above involves the solution of the secular equation, which in this case is given by the vanishing of the infinite determinant of $\boldsymbol{S}_g$ in (45). We recall that all of the parameters entering into $\boldsymbol{S}_g$ are assumed known, except for k_{x0} which is regarded as the unknown variable for any given frequency ω. In general, however, the quantities κ_m and c_{mn} (in the grating region) are not known explicitly, so that the determination of their values is part of the computation process for finding k_{x0}.

A first step in the programming of a computer routine for solving the transverse resonance (secular) relation is to provide a subroutine for the calculation of κ_m and c_{mn} for any given combination of k_a and k_{x0}. As discussed in Section III, such a subroutine is generally dependent on the specific grating structure, but it usually involves the calculation of a suitably truncated determinant of the infinite matrix defined in (22). After finding the eigenvalues κ_m of this truncated matrix, the pertinent Fourier coefficients c_{mn} can be determined from their defining relation (21). Of course, the accuracy of all κ_m and c_{mn} is dependent on the order of the truncated determinant. In general, this accuracy increases with the order; as the determinant is of the Hill's type, the truncation needs not be unduly large for the accuracies required by practical considerations. However, great care must be exercised when choosing the rows and columns of the truncated determinant because an improper choice may considerably degrade the ultimate accuracy that is obtained. This is particularly true for calculations involving waves at or near a Bragg condition in the grating region, i.e., for values of $\beta_0 d = N\pi (N = \pm 1, \pm 2, \pm 3, \cdots)$. A discussion on this question for the specific case of a sinusoidally modulated medium is given in [22, appendix]; it is expected that the considerations presented there apply also to a more general variation of periodic variations.

The subroutine for determining all required κ_m and c_{mn} is then introduced into the program that handles the calculation of k_{x0}. As was the case for the subroutine, the program for finding k_{x0} also involves the calculation of a suitably truncated determinant of an infinite matrix $\boldsymbol{S}_g$, which is again of the Hill's type. Hence the considerations for truncating $\boldsymbol{S}_g$ are similar to those for the subroutine mentioned above. However, when solving for k_{x0} by using (48) for the truncated determinant, the computer calculation (usually involving Newton's iteration method) may converge very slowly. This happens especially with configurations of the type shown in Fig. 1 for which the waveguiding process is primarily determined by the uniform layer rather than by the grating layer. In such cases, the calculation of k_{x0} is more easily and more accurately performed by utilizing another matrix $\boldsymbol{S}_f$ instead of $\boldsymbol{S}_g$.

This is obtained by noting from Fig. 5(b) that at $z = 0$ in the uniform layer, the field amplitudes $f_n^{(\pm)}$ are related by

$$\boldsymbol{f}^{(-)} = \hat{\boldsymbol{R}}_0 \boldsymbol{f}^{(+)} \tag{53}$$

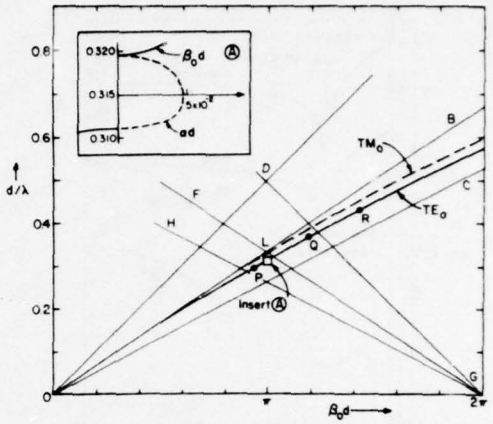

Fig. 6. Variation of $\beta_0 d$ for the fundamental TE and TM modes along a modulated layer as shown in Fig. 4 with $\epsilon_a = 1$, $\epsilon_g = 3.61$, $\epsilon_s = 2.25$, $M < 0.5$, and $t = 2d/\pi$. The insert shows the first stopband for $M = 0.08$.

where $\boldsymbol{f}^{(\pm)}$ are column vectors with elements $f_n^{(\pm)}$ and $\hat{\boldsymbol{R}}_0$ is given by $\bar{\boldsymbol{R}}_0$ in (47b) with the subscript s replaced by f in (46). On the other hand, at $z = -t_f$, the same amplitudes satisfy

$$f_n^{(+)} = \rho_n f_n^{(-)} \exp\,(i2k_{zn}^{(f)} t_f) \tag{54}$$

where ρ_n is given in (50). Inserting (54) into (53), we find

$$\boldsymbol{S}_f \boldsymbol{f}^{(+)} = [1 - \exp\,(i2\boldsymbol{k}_f t_f)\boldsymbol{R}_f \hat{\boldsymbol{R}}_0]\boldsymbol{f}^{(+)} = 0 \tag{55}$$

where $\boldsymbol{S}_f$ is defined by the matrix in the square brackets, $\exp\,(i2\boldsymbol{k}_f t_f)$ and $\boldsymbol{R}_f$ are diagonal matrices with elements $\delta_{mn} \exp\,(i2k_{zn}^{(f)} t_f)$ and $\delta_{mn}\rho_n$, respectively. Here $\det\,(\boldsymbol{S}_f) = 0$ expresses the transverse-resonance condition inside the film layer in a manner analogous to that whereby $\det\,(\boldsymbol{S}_g) = 0$ expresses this condition inside the grating layer.

By thus choosing a suitably truncated matrix $\boldsymbol{S}_f$ or $\boldsymbol{S}_g$, the computer program first finds k_{x0} by solving (48) or (55), after which the amplitudes a_n and s_n can be found by solving the simultaneous set of equations (38)–(41). The values of $k_{x0} = \beta_0 + i\alpha$, together with the magnitudes of all a_n and s_n, usually complete the information needed for the design of a particular dielectric grating structure.

To illustrate some of the results that can be obtained by the techniques discussed above, we present below several calculated curves for gratings of the type shown in Figs. 1(b) and 4.

The Brillouin diagram for a modulated layer is given in Fig. 6 for the lowest (fundamental) TE_0 and TM_0 modes. As predicted by the argument given in connection with Fig. 2, these dispersion curves show that the wavenumber β_0 is very closely equal to the value β_{sw} of the surface wave along a uniform ($M = 0$) layer. In fact, for values of $M \leq 0.5$, it is not possible to distinguish β_0 from β_{sw} on the scale of Fig. 6. In agreement with the theory of surface waves along uniform layers [21], the dispersion curves in Fig. 6 lie between the straight lines OB and OC

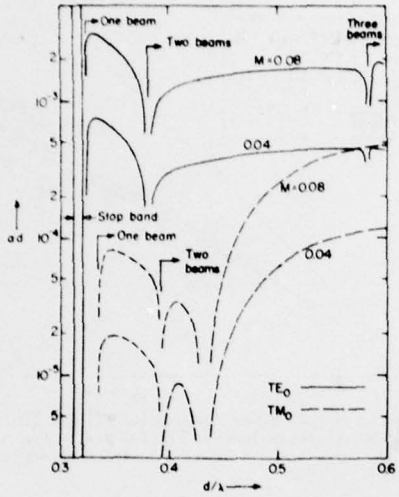

Fig. 7. Variation of the attenuation parameter α with frequency for the same grating as that in Fig. 6. The range shown allows for either a single beam in the substrate (e.g., point Q in Fig. 6) or for two beams, one each in the substrate and air regions (e.g., point R in Fig. 6). Inside the stopband, α becomes very large and reaches a peak which is well outside the vertical range shown.

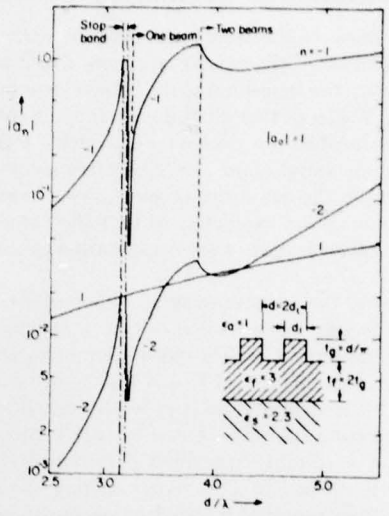

Fig. 8. Variation of the space-harmonic amplitudes a_n with frequency for the TE_0 mode along a rectangular grating.

through the origin, whose slope is given by $\cot^{-1}(\epsilon_s^{1/2})$ and $\cot^{-1}(\epsilon_g^{1/2})$, respectively.

The presence of periodicity manifests itself most strongly by causing stopbands at frequencies for which a Bragg condition $\beta_0 d = N\pi (N = \pm 1, \pm 2, \cdots)$ is satisfied. Such a stopband region is illustrated in Fig. 6 by insert A, which shows both $\beta_0 d$ and αd around $\beta_0 d = \pi$ in magnified form. For wavelengths λ inside this stopband, the field of the surface wave is in the form of a decaying standing-wave with respect to the x direction.

Besides producing stopbands, the presence of periodicity may also change the surface waves into leaky waves, as discussed in Section II. To assess this, we reflect the lines OB and OC about $\beta_0 d = \pi$ to obtain FG and HG. By taking into account the slopes of the various lines in conjunction with (6), we may verify that, for $j = a$ and s, all $k_{xn}^{(j)}$ are pure imaginary *inside* the triangular region OLG. However, $k_{x}^{(s)}$ is real *outside* this triangle, whereas both $k_{x,-1}^{(s)}$ and $k_{x,-1}^{(a)}$ are real outside the larger triangular region OLG. Thus at frequencies for which the operation point is inside the smaller triangle OLG (e.g., point P), the surface wave remains bound even if periodicity is present. As frequency increases and the operation point crosses the line FG (e.g., point Q), a radiation beam occurs in the substrate and the surface wave is changed to a leaky wave. For frequencies that are high enough so that the operating point is above the DG line (e.g., point R), radiation beams occur in both substrate and air regions.

The attenuation parameter α, which is due either to a stopband or to power leakage, is shown in Fig. 7. As frequency varies, α starts by being zero in the surface-wave region; however, α is nonzero and peaks strongly in the stopband region. This stopband behavior is of importance in the operation of distributed-feedback lasers and the maximum value of α determines the length required for effective lasing conditions. Outside the stopband α is nonzero if the frequency is high enough to produce radiation, i.e., the wave is leaky. As seen in Fig. 7, α varies slowly with frequency in the leaky-wave region, except in the vicinity of certain critical values of d/λ. These critical values of d/λ are associated with the presence of Wood's anomalies along gratings [24]; in the present case, these correspond to the onset of additional leaky-wave beams in the air or substrate regions. However, for TM modes, additional nulls may appear for α, which are due to a Brewster-angle phenomenon for a higher ($n \neq 0$) harmonic inside the grating layer. Such a case is shown by the null in α for TM_0 at about $d/\lambda = 0.43$.

For both surface-wave and leaky-wave applications, the amplitudes a_n are of great interest because their magnitudes determine the efficiency of devices that employ waves guided by periodic structures. We therefore show in Fig. 8 the variation of a_{-2}, a_{-1}, and a_1 (with $a_0 = 1$) for the fundamental TE_0 mode along a rectangular grating of the type shown in Fig. 1(b). We recall that a_n denotes the amplitude of the nth space harmonic at the air-grating boundary $z = t_g$. As the Brillouin diagram is basically similar to that already given in Fig. 6, it is omitted here, but its pertinent stopband and leaky wave regions are indicated in Fig. 8. It is noted that the curves for a_n undergo rapid variations close to the stopband edges. Also, we note that $|a_{-1}| = a_0 = 1$ and $|a_{-2}| = |a_1|$ within the stopband, in agreement with the fact that the field is a standing wave in the stopband.

Although some of the foregoing curves could have been calculated by the approximate techniques reported in the past [2]–[5], [7]–[9], [12], their accuracy should be checked by a rigorous method such as that presented here. To show the importance and the generality of the method discussed in this paper, we show in Fig. 9 the variation of α for the same grating as that of Fig. 8, except that now the wavelength λ is assumed fixed and the grating thickness

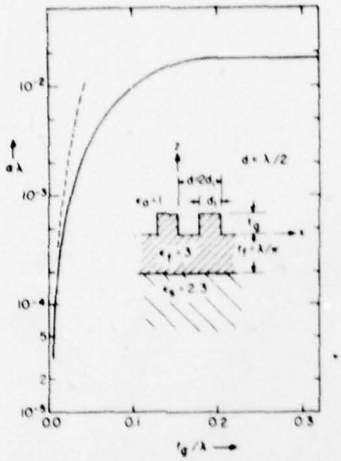

Fig. 9. Variation of α with the grating thickness t_g for the same grating as in Fig. 8. The solid curve shows the exact result whereas the dashed line refers to a result obtained by a perturbation analysis.

t_g varies. In this case, a perturbation analysis [5] would yield the dashed curve, for which α increases continuously with t_g. In contrast, our rigorous treatment yields the solid curve, which indicates that $\alpha\lambda$ reaches a saturation value close to 0.02 for values of $t_g/\lambda > 0.2$.

The behavior of the solid curve in Fig. 9 can easily be explained by noting that the basic surface wave along a uniform ($t_g = 0$) layer has an evanescent field in the air region. When increasing t_g from zero, we perturb this surface wave field by adding material on top of the uniform film of thickness t_f. At first, this material appears in a region with strong fields and therefore the effect on α is appreciable. However, as t_g increases further, the additional material appears in regions where the field has gradually decayed until, at about $t_g/\lambda = 0.2$, any further addition of material occurs in regions where the field is exponentially small. Consequently, the effect of increasing t_g beyond 0.2λ is negligible and α approaches a constant.

The above is only one example of the serious discrepancies that may occur between an exact result and that obtained by approximate techniques. Although the method presented here may be somewhat cumbersome to use, such a method is essential if one wishes to verify the validity of simpler but approximate results of unknown accuracy.

ACKNOWLEDGMENT

The authors wish to thank Prof. R. Petit, The University of Aix-Marseille III, France, for his constructive criticism of the first manuscript, and Mrs. Ida Tobiason for the patient and careful typing of the several versions of this work.

REFERENCES

[1] T. Tamir and H. L. Bertoni, "Lateral displacement of optical beams at multilayered and periodic structures," *J. Opt. Soc. Amer.*, vol. 61, pp. 1397–1413, Oct. 1971.
[2] L. L. Hope, "Theory of optical grating couplers," *Opt. Commun.*, vol. 5, pp. 179–182, June 1972.
[3] J. A. Harris, R. K. Winn, and D. G. Dalgoutte, "Theory and design of periodic couplers," *Appl. Opt.*, vol. 11, pp. 2234–2241, Oct. 1972.
[4] F. W. Dabby, A. Kestenbaum, and U. C. Paek, "Periodic dielectric waveguides," *Opt. Commun.*, vol. 6, Oct. 1972.
[5] K. Ogawa, W. S. C. Chang, B. L. Sopori, and F. J. Rosenbaum, "A theoretical analysis of etched grating couplers for integrated optics," *IEEE J. Quantum Electron. (Part I of Two Parts)*, vol. QE-9, pp. 29–42, Jan. 1973.
[6] S. T. Peng, T. Tamir, and H. L. Bertoni, "Leaky-wave analysis of optical periodic couplers," *Electron. Lett.*, vol. 9, pp. 150–152, Mar. 1973.
[7] C. Elachi and C. Yeh, "Frequency selective coupler for integrated optics systems," *Opt. Commun.*, vol. 7, pp. 201–204, Mar. 1973.
[8] K. Sakuda and A. Yariv, "Analysis of optical propagation in a corrugated dielectric waveguide," *Opt. Commun.*, vol. 8, pp. 1–4, May 1973.
[9] H. Stoll and A. Yariv, "Coupled-mode analysis of periodic dielectric waveguides," *Opt. Commun.*, vol. 8, pp. 5–8, May 1973.
[10] (a) N. Neviere, R. Petit, and M. Cadilhac, "About the theory of optical grating coupler-waveguide systems," *Opt. Commun.*, vol. 8, pp. 113–117, June 1973.
(b) M. Neviere, P. Vincent, R. Petit, and M. Cadilhac, "Systematic study of resonance of holographic thin film couplers," *Opt. Commun.*, vol. 9, pp. 48–53, Sept. 1973.
(c) ——, "Determination of the coupling coefficient of a holographic thin film coupler," *Opt. Commun.*, vol. 9, pp. 240–245, Nov. 1973.
[11] C. Elachi and C. Yeh, "Periodic structures in integrated optics," *J. Appl. Phys.*, vol. 44, pp. 3146–3152, July 1973.
[12] K. Ogawa and W. S. C. Chang, "Analysis of holographic thin film grating coupler," *Appl. Opt.*, vol. 12, pp. 2167–2171, Sept. 1973.
[13] S. T. Peng, H. L. Bertoni, and T. Tamir, "Analysis of periodic thin-film structures with rectangular profile," *Opt. Commun.*, vol. 10, pp. 91–94, Jan. 1974.
[14] S. T. Peng, T. Tamir, and H. L. Bertoni, "Analysis of thick-grating beam couplers," in *Digest Tech. Papers, Topical Meeting on Integrated Optics*, pp. TuB8-1–TuB8-4, Jan. 1974.
[15] L. V. Kantorovich and V. I. Krilov, *Appropriate Methods of Higher Analysis*. New York: Interscience, 1958, sec. 1.3, p. 26.
[16] T. Tamir, H. C. Wang, and A. A. Oliner, "Wave propagation in sinusoidally stratified dielectric media," *IEEE Trans. Microwave Theory Tech.*, vol. MTT-12, pp. 323–335, May 1964.
[17] H. C. Wang, "Electromagnetic wave propagation along a sinusoidally stratified dielectric slab," Ph.D. dissertation, Polytechnic Institute of Brooklyn, New York, N.Y., 1965.
[18] C. Yeh, K. F. Casey, and Z. A. Kaprelian, "Transverse magnetic wave propagation in sinusoidally stratified dielectric media," *IEEE Trans. Microwave Theory Tech.*, vol. MTT-13, pp. 297–302, May 1965.
[19] S. T. Peng and A. Hessel, "Generalized continued fractions in electromagnetic problems," presented at the URSI Meeting, Boulder, Colo., Aug. 1973, to be published.
[20] L. R. Lewis and A. Hessel, "Propagation characteristics of periodic arrays of dielectric slabs," *IEEE Trans. Microwave Theory Tech.*, vol. MTT-19, pp. 276–286, Mar. 1971.
[21] T. Tamir, "Inhomogeneous wave types at planar interfaces: II Surface waves," *Optik*, vol. 37, pp. 204–228, Sept. 1973.
[22] ——, "Scattering of electromagnetic waves by a sinusoidally-stratified half space, Part II: diffraction aspects at the Rayleigh and Bragg wavelengths," *Can. J. Phys.*, vol. 44, pp. 2461–2494, Oct. 1966.
[23] S. T. Peng and T. Tamir "Effects of groove profile on the performance of dielectric grating couplers," in *Proc. Symp. Optical and Acoustical Micro-Electronics*. Brooklyn, N.Y.: Polytechnic Press, 1974.
[24] A. Hessel and A. A. Oliner, "A new theory of Wood's anomalies on optical gratings," *Appl. Opt.*, vol. 4, pp. 1275–97, Oct. 1965.
[25] R. E. Collin and F. J. Zucker, Eds., *Antenna Theory*, vol. 2. New York: McGraw-Hill, 1969, sec. 19.10, p. 203.

Reprinted, with permission, from IEEE TRANSACTIONS on Microwave Theory and Techniques, January 1975, Vol. MTT-23, No. 1 pp. 123-133.